

# Improving the VANET Vehicles' Localization Accuracy Using GPS Receiver in Multipath Environments

by

Nabil Drawil

A thesis  
presented to the University of Waterloo  
in fulfilment of the  
thesis requirement for the degree of  
Master of Applied Science  
in  
Electrical and Computer Engineering

Waterloo, Ontario, Canada, 2007

© Nabil Drawil 2007

I hereby declare that I am the sole author of this thesis. This is a true copy of the thesis, including any required final revisions, as accepted by my examiners.

I understand that my thesis may be made electronically available to the public.

# Abstract

The Vehicular Ad-hoc Network (VANET) has been studied in many fields since it has the ability to provide a variety of services, such as detecting oncoming collisions and providing warning signals to alert the driver. The services provided by VANET are often based on collaboration among vehicles that are equipped with relatively simple motion sensors and GPS units. Awareness of its precise location is vital to every vehicle in VANET so that it can provide accurate data to its peers. Currently, typical localization techniques integrate GPS receiver data and measurements of the vehicle's motion. However, when the vehicle passes through an environment that creates a multipath effect, these techniques fail to produce the high localization accuracy that they attain in open environments. Unfortunately, vehicles often travel in environments that cause a multipath effect, such as areas with high buildings, trees, or tunnels. The goal of this research is to minimize the multipath effect with respect to the localization accuracy of vehicles in VANET.

The proposed technique first detects whether there is a noise in the vehicle location estimate that is caused by the multipath effect using neural network technique. It next takes advantage of the communications among the VANET vehicles in order to obtain more information from the vehicle's neighbours, such as distances from target vehicle and their location estimates. The proposed technique integrates all these pieces of information with the vehicle's own data and applies optimization techniques in order to minimize the location estimate error.

The new techniques presented in this thesis decrease the error in the location estimate by 53% in the best cases, and in the worst case produce almost the same error in the location estimate as the traditional technique. Moreover, the simulation results show that 60% of the vehicles in VANET decrease the error in their location estimates by more than 13.8%.

# Acknowledgments

I would like to thank Dr. Otman Basir, my supervisor, who offered me the opportunity to be a graduate student at the University of Waterloo and gave me the guidance and inspiration to start this thesis.

I would like to thank the Libyan Ministry of Education who sponsored me during my study.

I am also grateful to all the people who helped me directly or indirectly during my research.

# Dedication

I would like to dedicate this thesis to my parents, who started and nurtured my academic interests; to my brothers and sisters, who support and encourage me all the time; and to my wife and my daughter, who gave me the ultimate desire to finish this work.

# Contents

|          |   |           |
|----------|---|-----------|
| <b>1</b> | <b>Introduction</b>   | <b>1</b>  |
| 1.1      | Research Motivation . . . . .   | 2         |
| 1.2      | Research Objective . . . . .  | 4         |
| 1.3      | Thesis Outline . . . . .  | 5         |
| <b>2</b> | <b>Background and Literature Review</b>                                   | <b>6</b>  |
| 2.1      | Global Positioning Systems . . . . .                                      | 6         |
| 2.2      | An Overview of a Differential GPS . . . . .                               | 9         |
| 2.3      | Dead Reckoning System . . . . .   | 10        |
| 2.4      | Literature Review . . . . .   | 11        |
| <b>3</b> | <b>Inter Vehicle Communication Assisted Localization Solution(IVCALS)</b> | <b>17</b> |
| 3.1      | Formulation . . . . .   | 17        |
| 3.2      | Kalman Filter a Location/Data Tool . . . . .                              | 24        |
| 3.3      | Improving Localization in a Multipath Environment . . . . .               | 30        |
| 3.3.1    | Evaluation of Uncertainty in Localization . . . . .                       | 31        |
| 3.3.2    | Detection of the Multipath Effect Using NNET . . . . .                    | 34        |
| 3.3.3    | An Algorithm for Improving the Location Estimate . . . . .                | 37        |
| 3.3.4    | The Least Square Minimization of the Localization Error . . . . .         | 40        |
| 3.3.5    | The Nelder-Mead Method of Optimization . . . . .                          | 41        |
| 3.4      | Summary . . . . .   | 45        |

|          |   |           |
|----------|---|-----------|
| <b>4</b> | <b>Experimental Results</b>                             | <b>46</b> |
| 4.1      | Setup Kalman Filter Implementation . . . . .            | 47        |
| 4.2      | Simulation Scenario . . . . .                           | 51        |
| 4.3      | Results . . . . .                                       | 54        |
| 4.3.1    | Analyzing the IVCALS Technique in the Multipath Regions | 60        |
| 4.3.2    | The Adaptive IVCALS Technique . . . . .                 | 65        |
| 4.4      | The Results of the Adaptive IVCALS Technique . . . . .  | 70        |
| 4.4.1    | Comparison of the Techniques and Experiments . . . . .  | 72        |
| <b>5</b> | <b>Conclusions and Future Work</b>                      | <b>81</b> |
| 5.1      | Conclusions . . . . .                                   | 81        |
| 5.2      | Future Work . . . . .                                   | 85        |
| 5.2.1    | 3D Coordinates . . . . .                                | 85        |
| 5.2.2    | MAC and Network Layers . . . . .                        | 85        |
| 5.2.3    | Embedded systems' design . . . . .                      | 85        |

# List of Figures

|     |   |    |
|-----|---|----|
| 2.1 | GPS satellites arranged in six orbital planes. . . . .                          | 7  |
| 2.2 | Differential GPS receivers. . . . .   | 10 |
| 3.1 | Vehicular ad hoc network (VANET) . . . . .                                      | 18 |
| 3.2 | The Multipath effect on the GPS receiver . . . . .                              | 20 |
| 3.3 | Block diagram of the proposed technique . . . . .                               | 22 |
| 3.4 | The discrete Kalman Filter loop. . . . .  | 29 |
| 3.5 | Architecture of a general neural network. . . . .                               | 35 |
| 3.6 | Neural network for detecting the multipath effect. . . . .                      | 36 |
| 3.7 | The flowchart of the algorithm for improving the location estimate. . . . .     | 39 |
| 3.8 | The flow chart of the Nelder-Mead optimization method. . . . .                  | 43 |
| 3.9 | One step of the Nelder-Mead simplex method in $\mathbb{R}^3$ . . . . .          | 44 |
| 4.1 | Example of localization for one vehicle in open area . . . . .                  | 49 |
| 4.2 | Example of localization for one vehicle in multipath environment . . . . .      | 50 |
| 4.3 | The multipath effect extends to the open area environment . . . . .             | 52 |
| 4.4 | VANET simulation scenario. . . . .  | 53 |
| 4.5 | Simulation of localization using the Kalman Filter . . . . .                    | 55 |
| 4.6 | Simulation of localization using the IVCALS technique . . . . .                 | 58 |
| 4.7 | 3D representation of the optimization function in the ideal case. . . . .       | 62 |
| 4.8 | Contour representation of the optimization problem in the ideal case. . . . .   | 63 |
| 4.9 | Example of the solution for the optimization problem in the ideal case. . . . . | 64 |



|      |   |    |
|------|---|----|
| 4.10 | Example of the effect of the unaccuarte reference vehicls . . . . .   | 66 |
| 4.11 | 3D representation of the optimization Problem in the real case. . . . | 67 |
| 4.12 | Contour diagram for the case of more than on global minimum . . . .   | 68 |
| 4.13 | The adaptive IVCALS technique . . . . .                               | 71 |
| 4.14 | Simulation for localization using the adaptive IVCALS technique . .   | 73 |
| 4.15 | Comparing the three techniques w.r.t. the std. deviation of the error | 75 |
| 4.16 | Comparison among the three techniques vs the mean error . . . . .     | 76 |
| 4.17 | Comparison of the IVCALS and the adaptive IVCALS techniques .         | 79 |
| 4.18 | Performance measures . . . . .  | 80 |

# List of Tables

|     |  |    |
|-----|--|----|
| 4.1 | Error statistics for the localization using the Kalman Filter. . . . . | 56 |
| 4.2 | Error statistics for the localization using IVCALS tehcnique. . . . .  | 60 |
| 4.3 | statistics for the localization using the adaptive IVCALS technique.   | 72 |

# Chapter 1

## Introduction

During the last two decades, wireless network technology has progressed at a very fast rate. Improvements have played an essential role in opening doors for researchers to consider new solutions for various applications. Cellular, Ad hoc, and wireless sensor networks are examples of recent wireless network technologies that have been used in telecommunication, monitoring, remote sensing, security, location estimation, and tracking systems. The later two applications have attracted the attention of many governmental and non-governmental organizations because location awareness can be deployed in numerous services. A vehicular ad hoc network (VANET), a type of wireless network, is able to provide many communication services via the collaboration of the vehicles in the network. However, the accuracy of its localization is not satisfactory for some applications. In this thesis, a new technique for improving the localization process in VANET is proposed. This chap-

ter describes the motivation and the objectives of this research and then explains the outline of the thesis.

## 1.1 Research Motivation

VANET has been proposed as an automated solution to many problems related to transportation, highway safety, and driving assistance. For instance, most taxi companies respond to customer calls in a way that results in a great deal of fuel consumption, air pollution, and wasted time. Since it has the ability to relay information through a network of vehicles, VANET could assign the closest free taxi to serve a customer which could minimize the above drawbacks.

Emergency systems also offer a vital service that requires location information. When an accident occurs, this information can help the system make the right decision and request the nearest emergency centre to take action. For this reason the Federal Communications Commission (FCC) mandates that U.S. mobile phone companies provide 911 operators with the location information for millions of wireless subscribers [1]. However, in many cases, the accident victims are not able to call 911, for instance, in severe vehicular accidents. In the U.S. alone, the number of auto accidents in 2005 was about 6,420,000 [2]. Such accidents provide

a compelling reason for having an automatic emergency system on each vehicle, so that an emergency message can be sent automatically from the location of the accident to the closest emergency centre. This message should also warn other vehicles travelling toward the accident about related traffic congestion.

VANET's facilitation of communication among vehicles can help in solving the problems described above. A great deal of research has been done in this area and has proven that location estimation (localization) is a building block for many VANET and other systems, such as the ones reported in [3, 4, 5, 6]. These networks consist of hundreds or even tens of thousands of nodes. Depending on the type of network, the nodes could be vehicles or small inexpensive sensors. Each node in the network communicates with its neighbours within a limited radio range. The way nodes relay information is controlled by routing protocols, which are often location based. Although VANET and wireless sensor networks have some characteristics in common, such as the randomness of the availability of a neighbour and the changes in network topology from one time to another, they are different with respect to energy consumption constraints. Consequently, one may consider that a satellite-based global positioning system (GPS) is the best way to localize nodes in VANET since every vehicle has more than enough energy to supply a GPS receiver.

However, using a GPS receiver as a stand-alone localization technique has drawbacks. A regular GPS used without any specialized equipment can be less accurate, e.g., they are accurate only up to 5 to 10 meters in outdoor environment or open area. In addition, a GPS is not applicable in locations where no line of sight exists, e.g., in a tunnel. Therefore, integrating a GPS receiver with other localization methods is well worth the efforts invested by many researchers, such as [7, 8, 9, 10, 11], and it is still an unsolved problem.

## 1.2 Research Objective

The objective of this thesis is to improve the accuracy of localization techniques in VANET so that it can be used as a robust system during long GPS outages. To accomplish this objective, the following techniques have been developed and tested:

- The Kalman Filter integrates the Inertial Navigation System on a vehicle with the GPS receiver in order to overcome most of the individual drawbacks in the two systems when they operate independently.
- The optimization method minimizes Kalman Filter positioning errors by using information extracted from the communication among vehicles.
- The updating technique feeds the localization corrections back to the Kalman Filter, which compensates for the GPS outages.

## 1.3 Thesis Outline

Related research and background are presented in Chapter 2, in which the different localization methods in VANET are discussed. Chapter 3 describes the Kalman Filter and the formulation of the optimization and updating techniques that help improving the location estimates. Chapter 4 contains the experimental work and the results that demonstrate the improvements in the location estimates using the techniques mentioned in Chapter 3. Finally, Chapter 5 presents the conclusions of the thesis and recommendations for future work.

# Chapter 2

## Background and Literature Review

### 2.1 Global Positioning Systems

GPS is a positioning system that has been developed and operated by the U.S. Department of Defence [12]. A GPS system is formed from a network of satellites that transmit Continuous coded information, which makes it possible to identify locations on Earth by measuring distances from the satellites; moreover, the receiver also has the ability to obtain information about its velocity and direction. A GPS network consists of 24 satellites arranged in six orbital planes, as depicted in Figure 2.1, so that at any given time a minimum of five satellites can be observed by GPS receivers at any location in the world. Different types of GPS receivers have been developed for many applications according to the accuracy required.



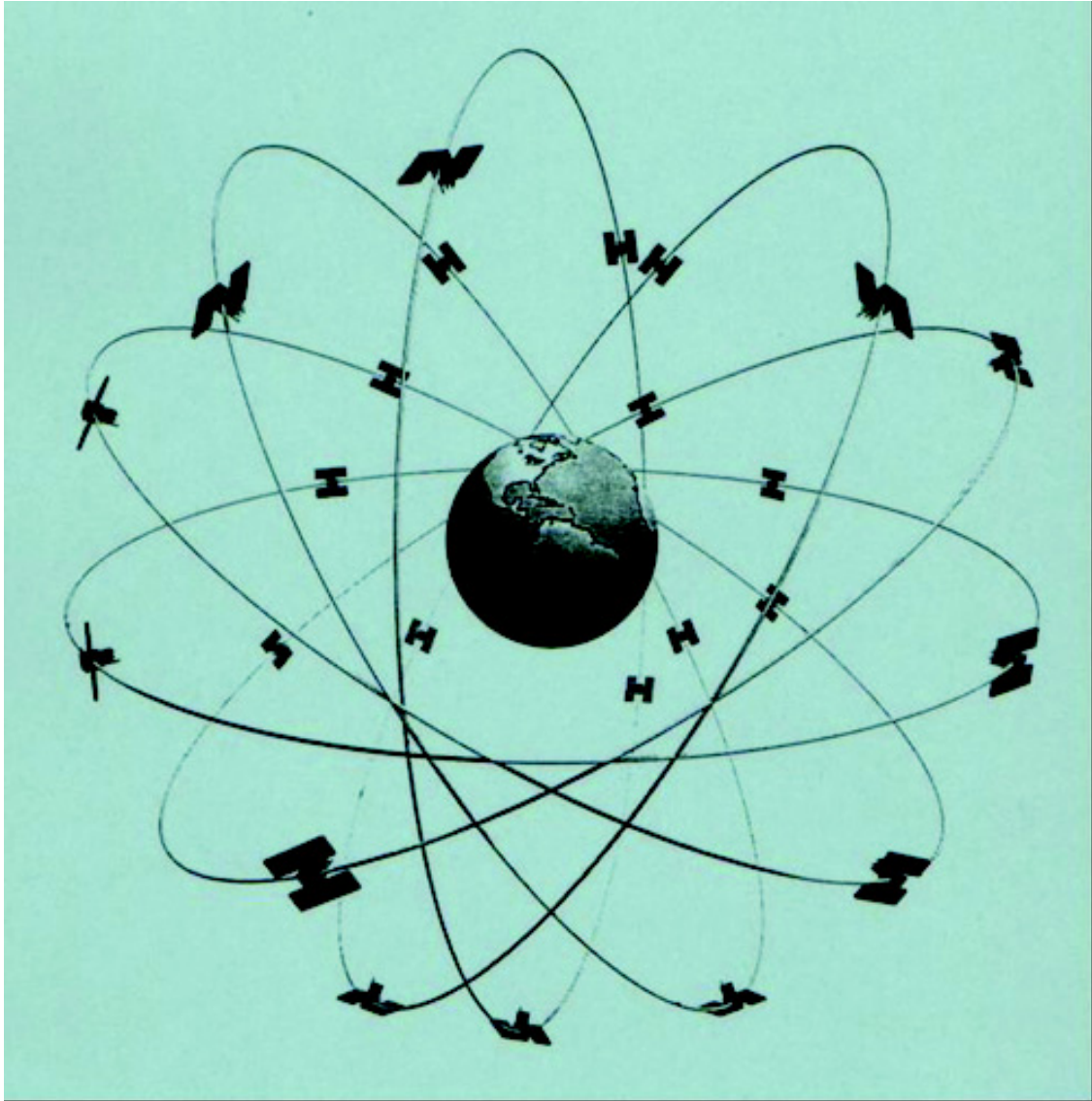


Figure 2.1: GPS satellites arranged in six orbital planes.

In fact, basic GPS receivers often have four radio channels so that the receiver can observe four GPS satellites at once and obtain a pseudo-range measurement from each satellite signal. Leva in [13] and Hoshen in [14] show two different techniques by which a GPS receiver can compute its location from four pseudo-range measurements, minimum required for localization in three dimensions. However, if one of the GPS satellites' signals does not appear, it is hard to identify the location of the GPS receiver from only three measurements. Therefore, the more advanced receivers have been developed to have six or more radio channels. The extra channels keep observing other GPS satellites and put their information in reserve, to use in case one or more of the four signals is missing.

Unfortunately, this increase in the complexity of the hardware in the GPS receiver adds to the cost but does not guarantee accurate location measurements. The pseudo-range measurement includes many errors which decreases the accuracy to a range of 10 to 50 meters. These errors can be categorized as global or local errors. Global errors affect the receiver's measurements by values that vary from one area to another because of ionospheric delays, tropospheric delays, ephemeris, and satellite clocks. Selective availability (SA) is not mentioned here because it has been eliminated [15] since the first of May 2001 and no longer affects GPS measurements. Local errors can be caused by multipath effects, by not being in

the line of sight, or by the receiver hardware itself. More details about global and local GPS measurement errors are described in [16].

## 2.2 An Overview of a Differential GPS

It is possible to avoid most global errors and obtain accurate location measurements by using a differential GPS receiver (DGPS). A DGPS consists of two receivers observing the same GPS satellites. One of these receivers is stationary and the other one, which is used to measure the locations, roves. The stationary receiver resides at a known location and obtains the pseudo-range from the satellites' signals, so it identifies a global error by comparing the measurements with its location. Next, the stationary receiver transmits the global error correction to the roving receiver so that the roving one can correct its measurements. In the best cases, the accuracy increases to the level of tens of centimetres when a DGPS is used. However, this type of receiver has drawbacks, such as the cost of the communication channels between the stationary receiver and the roving receiver(s) and the cost of the hardware. Moreover, DGPS receivers must be under the coverage of the same GPS satellites in order to be correlated, i.e., having the same global error. Hence, this requirement ties up the roving receiver and allow it to move only in a bounded area. However, the DGPS can not correct local errors since the multipath effects happen immediately

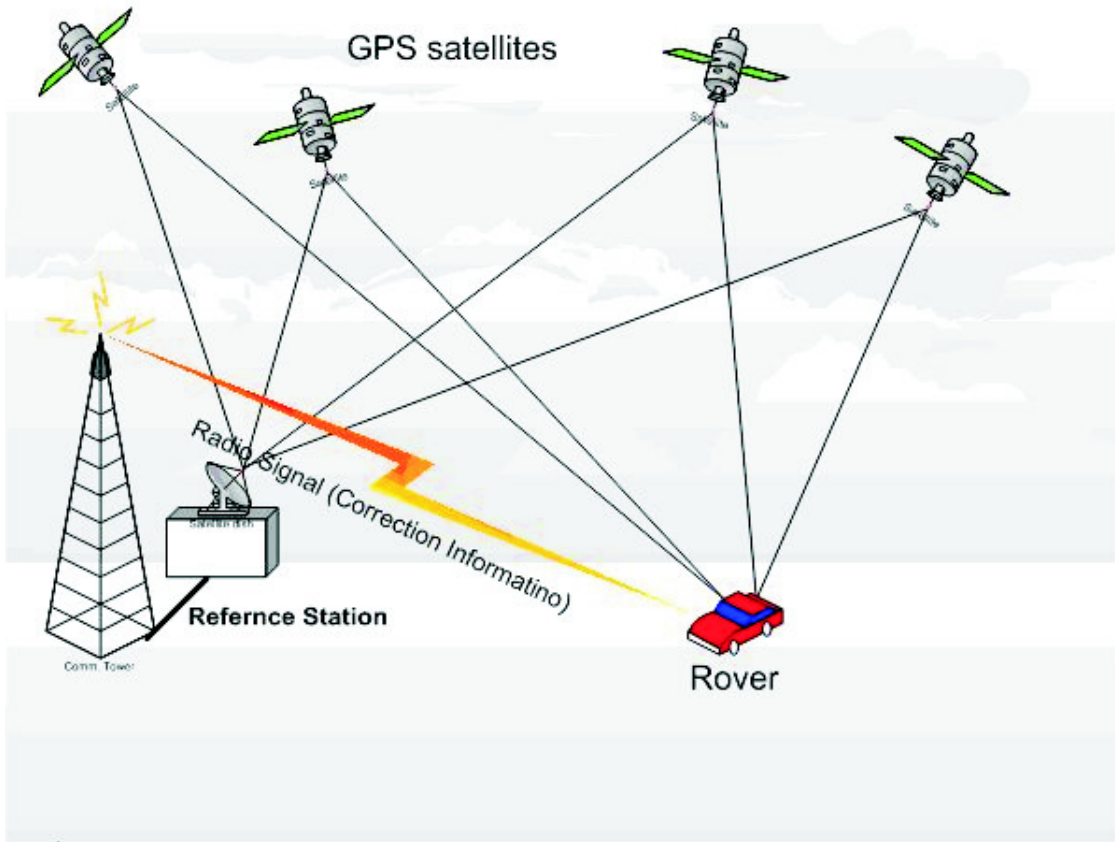


Figure 2.2: Differential GPS receivers.

around the roving receiver, and the hardware errors are individual.

## 2.3 Dead Reckoning System

Another method of localization, called Dead Reckoning System (DRS), has been adopted in some applications. In this technique, the new location estimation de-

depends on how far an object has moved from a known place given the directions and distances traveled over small periods of time. Since this technique is simple and inexpensive, it is the choice for many applications; however, it has a crucial disadvantage in that the errors in the measurements of the direction and/or the distance affect the final location estimation. In other words, the measurement errors accumulate over the total period of time. Thus, the Dead Reckoning technique is recommended for use only over short periods of time.

## 2.4 Literature Review

GPS and DRS techniques are both commonly used in vehicle navigation systems. However, they suffer from different drawbacks. Integrating the two methods is one approach to developing a superior technique. Many researchers have been motivated by this idea and have looked at it from different points of view. In [7], W. W. Kao proposed combining the standard GPS receiver and a DRS in one navigation system so that the GPS fixes the accumulated error caused by the DRS, when the GPS measurement is not available, and the DRS estimates the location using sensors such as wheel odometers, flux-gate compass, gyroscope, and accelerometer. Similarly, Qi Honghui et al. stated in [9] that it is possible to integrate the GPS reading with the Inertial Navigation System (INS) by means of a Kalman Filter.

In addition, the authors attempted to eliminate the computational complexity of the Extended Kalman Filter by preprocessing the INS measurements and inputting them to the Kalman Filter as a linear component. However, the time consumed during the preprocessing of the INS-sensed data remains. on hte other hand, D. Bouvet and G. Garcia proposed a Real-Time Kinematic Global Positioning System (RTK GPS) using an Extended Kalman Filter [8]. They identified GPS latency that could be caused by the time required for the satellite signals to travel to the Earth, by the time required for the computation of the location, or by one or more of the GPS satellites changing while the signals being received. These delays might corrupt the synchronization of the reading of the sensors, especially when they are used in the control loop of a moving vehicle to estimate its location using a high-precision system.

In [10], R. Sharaf et al. have chosen the Artificial Neural Network (ANN) as a tool for recognizing errors and noises in the GPS/INS measurements. They reported that since the ANN training process is often time-consuming, they used a Radial Basis Function (RBF) neural network, which is relatively fast. The work in [10] is quite similar to that in [8] in that preprocessing operations must be performed on the measurements before they can be fused.

Recent work has been done by S. Rezaei and R. Sengupta [11] to integrate the INS with a DGPS. Because of the nonlinearity in their dynamic model, they used an Extended Kalman Filter as a fusion tool. they reported that their filter was able to recognize lanes and turns at about 100 m when the system relied on the dynamic model more than on the GPS measurements, because a GPS has a slow sampling frequency. On the other hand, they ignored the multipath effect because the field used in the experiment contained no very high building or trees.

It can thus be concluded that even with the most advanced and expensive GPS/DGPS, it is essential to integrate GPS measurements with other measurements such those from an INS to improve the localization process. None of the mentioned papers was able to overcome the problem of losing the satellite signals; therefore, it is better to find another source of information that can help with the goal of improving location estimation.

With respect to VANET, many researchers have proposed GPS as a localization technique for use with this system. However, in many applications it is not a satisfactory tool for location estimation. For example, a monitoring system that charges vehicles for using a specific highway, such as Highway 407, ought to discriminate between those vehicles on that highway and others outside the highway,

for instance on suburban roads beside the highway. Such a system requires highly accurate location estimation. Integrating a GPS with an INS does not achieving high accuracy or a nearly fault-free system. Moreover, a DGPS has constraints such as the need for infrastructure, the cost of the communication channels, and the limited geographical area.

Other publications have focused on GPS-less techniques for localization, such as [17]. These techniques rely mainly on estimating the distance between every two nodes, a method inspired by the localization approaches used in cellular networks [18, 19, 20]. These approaches are based on one of the radio-location methods: Time of Arrival (TOA), Angle of Arrival (AOA), Received Signal Strength (RSS), or Time Difference of Arrival (TDOA) [21]. Once the distances are obtained, the nodes with unknown locations perform triangulation or build a relative coordination system. However, the radio-location methods suffers from two types of errors: the multipath effect or non-line-of-sight (NLOS), and hardware measurement errors. In [17], S. Capkun et al. first mitigate the NLOS using the algorithm proposed in [20], which is called *Rwgh*; they then create local coordination system for each node so that every node has a list of its immediate neighbours and their position relative to that node. By broadcasting these lists to their immediate neighbours, nodes record the neighbours two hops away and their positions. The process is repeated



for the three-hops neighbours, and so on. Although S. Capkun et al. report that the system attains enough stability and location accuracy, despite the error in the range distance using the TOA method, the system does not suit VANET because of the speed of the nodes in VANET and the maintenance of the neighbours which is expected to produce more bandwidth communication. On the other hand, this method is appropriate for MANET, which is somewhat slower than VANET.

For VANET, A. Benslimane introduces in [22] a new method of localizing vehicles unequipped with a GPS receiver or those whose location can not be determined because the satellite signals are lost, for instance, in a tunnel. In this technique the unequipped vehicles rely on vehicles that are equipped with GPS and able to determine their locations. Since, depending on the radio range, every two vehicles are able to communicate within a limited distance, they can measure the distance between themselves using one of the radio-location methods presented in [21]. By finding three neighbours closest to the unequipped vehicle, its position can be computed using triangulation. Other cases, when fewer than three neighbours are available, are discussed thoroughly in [22]. The author reports that when there are as many as 40% of the total number of the vehicles in the network are equipped, the system can be optimal; nevertheless, no mention is made of the accuracy or even the type of GPS receiver used on the equipped vehicles. Conceivably, precision

in such applications is not a concern.

The idea proposed in this thesis is to take advantage of all the research mentioned and develop a new localization technique in VANET that will increase the accuracy of the location estimation so that it will be precise enough for most spatial systems. The concern is not just to help safety systems avoid vehicles pile-ups at an accident site by sending a warning message about a jam ahead; instead, the aim is to pinpoint a specific vehicle on a highway or street map with a very high degree of accuracy, so that the side of an intersection on which it is located can be determined.

Specifically, using Kalman Filter to integrate a GPS reading with the measurements from other vehicle sensors is very beneficial since fusing the measurement sets overcomes some of the faults indicated in previous paragraphs. However, a Kalman Filter has drawbacks, mainly because of losing satellite signals and the multipath effect. Using VANET's facility for communication among nodes may provide another piece of information about the distances between every two nodes that may help compensate for losing satellite signals.

# Chapter 3

## Inter Vehicle Communication Assisted Localization Solution(IVCALS)

### 3.1 Formulation

In this thesis, it is assumed that VANET is an ad-hoc wireless network that is comprised of vehicles equipped with a GPS receiver, an Inertial Navigation System (INS), and a radio transceiver. The vehicles resemble mobile nodes in an ad hoc wireless network. In this thesis, the target vehicle in the network is marked as  $V_o$ , and the other nodes are marked as  $V_i$ , where  $i=1,2,3\dots n$ .  $n$  represents the number of the immediate neighbours. Every node can communicate directly with other nodes within a radius  $R$  that depends mainly on the type of transceiver installed in the vehicles. Since the nodes are mobile, they have speeds and directions, marked  $S_{t,i}$  and  $\theta_{t,i}$  respectively, where  $i$  signifies the index of a specific node and  $t$  indi-

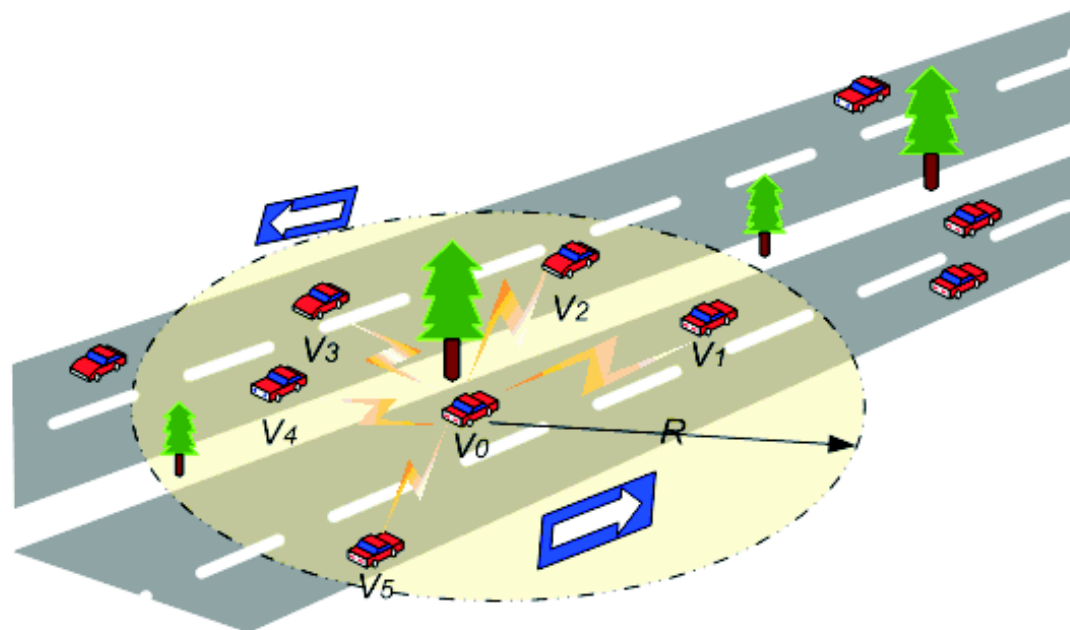


Figure 3.1: Vehicular ad hoc network (VANET)

icates the time; the presumption is that the speed and direction may change over time. Moreover, it is assumed that all measurements are taken in discrete intervals indexed by  $t$ .

Every node in the network is trying to estimate its location via the Kalman Filter technique. A Kalman Filter integrates the Inertial Navigation System and the GPS measurements. While the GPS reading periodically corrects the INS error, INS measurements help estimate the location in the absence of satellite signals or

until the system obtains the next GPS reading. Although a Kalman Filter combines the two methods and gains the advantages of each one, a localization error  $E_{t,i}$  occurs every time a node estimates its position. This error is caused by a GPS measurement error and an INS measurement error. This drawback leads to a quick deviation from the real vehicle location during a long absence of satellite signals or in the case of severe multipath effects. In [23], work has been focused on improving the INS measurement equipment in order to increase the accuracy of localization in the absence of the GPS reading; however, such a system will not be reliable if the absence is experienced over a long period of time.

In other words,  $E_{t,i}$  would not be relatively large if the vehicle does not experience any loss of GPS signals. However, other factors might affect  $E_{t,i}$ , such as global, and local GPS measurement errors (the geographic location and the surrounding environment). For a group of vehicles, such as those in Figure 3.2, the global GPS error is almost the same since they are covered by the same GPS satellites. On the other hand, the local GPS receiver error is different from one vehicle to another because it depends on the environment surrounding each vehicle. As a result, for short periods of time, the change in  $E_{t,i}$  is dominated by the local error since most vehicles travel quickly; the surrounding environment changes rapidly.

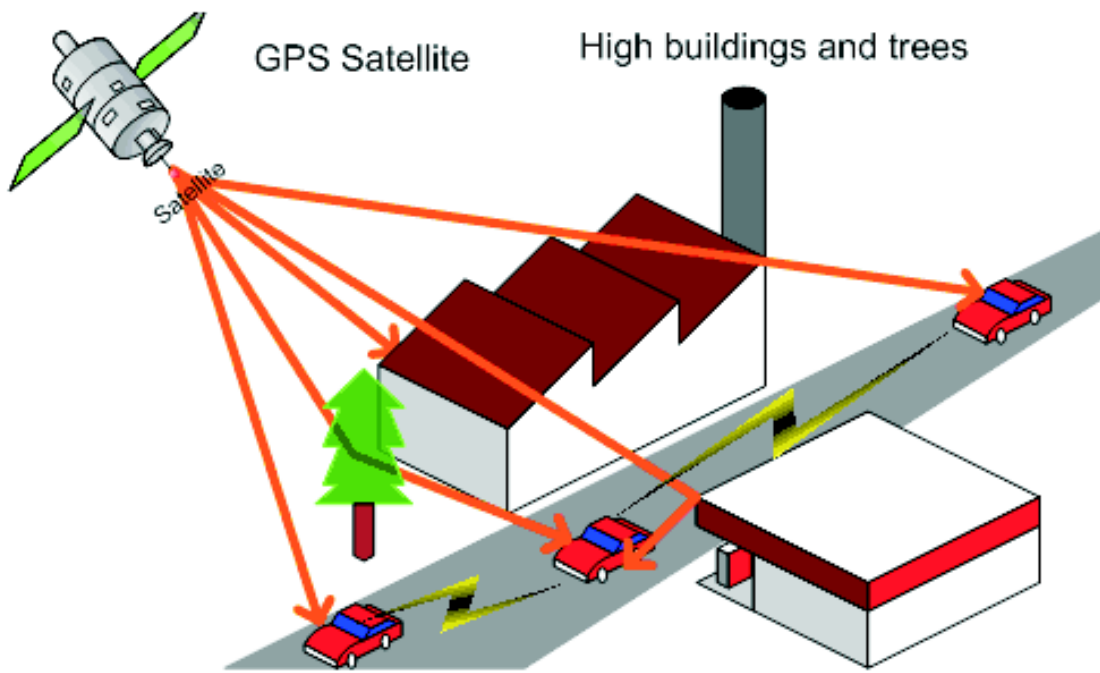


Figure 3.2: Multipath effect, when satellite signals are reflected off of high buildings and/or trees.

From an early work focused on analysing and modelling the errors of associated with different types of GPS receivers, in [24], J. Rankin was able to model most GPS global errors; however, Cannon et al. mentioned in [25] that the multipath effect has a random behaviour. Logically, this is true because one can not anticipate the specific environment that any vehicle may pass through during a 24-hour period. For example, some vehicles commute every day through an open area with almost no multipath effect. Another group of vehicles spend all their time travelling inside large cities, where satellite signals are reflected off of or are blocked by huge buildings, and therefore exposed to a multipath effect most of the time. Still other vehicles experience both of these cases.

The approach proposed in this thesis introduces an additional optimization operation to the traditional systems. The optimization operation is applied to the output of a Kalman Filter in order to increase the accuracy of the localization. The diagram of the new approach, which is discussed in the next sections, is depicted in Figure 3.3.

This approach aims to extract information from the nodes in the vicinity of any target vehicle by taking advantage of the communication among nodes in VANET. This information includes distances between every vehicle and its neighbours, how

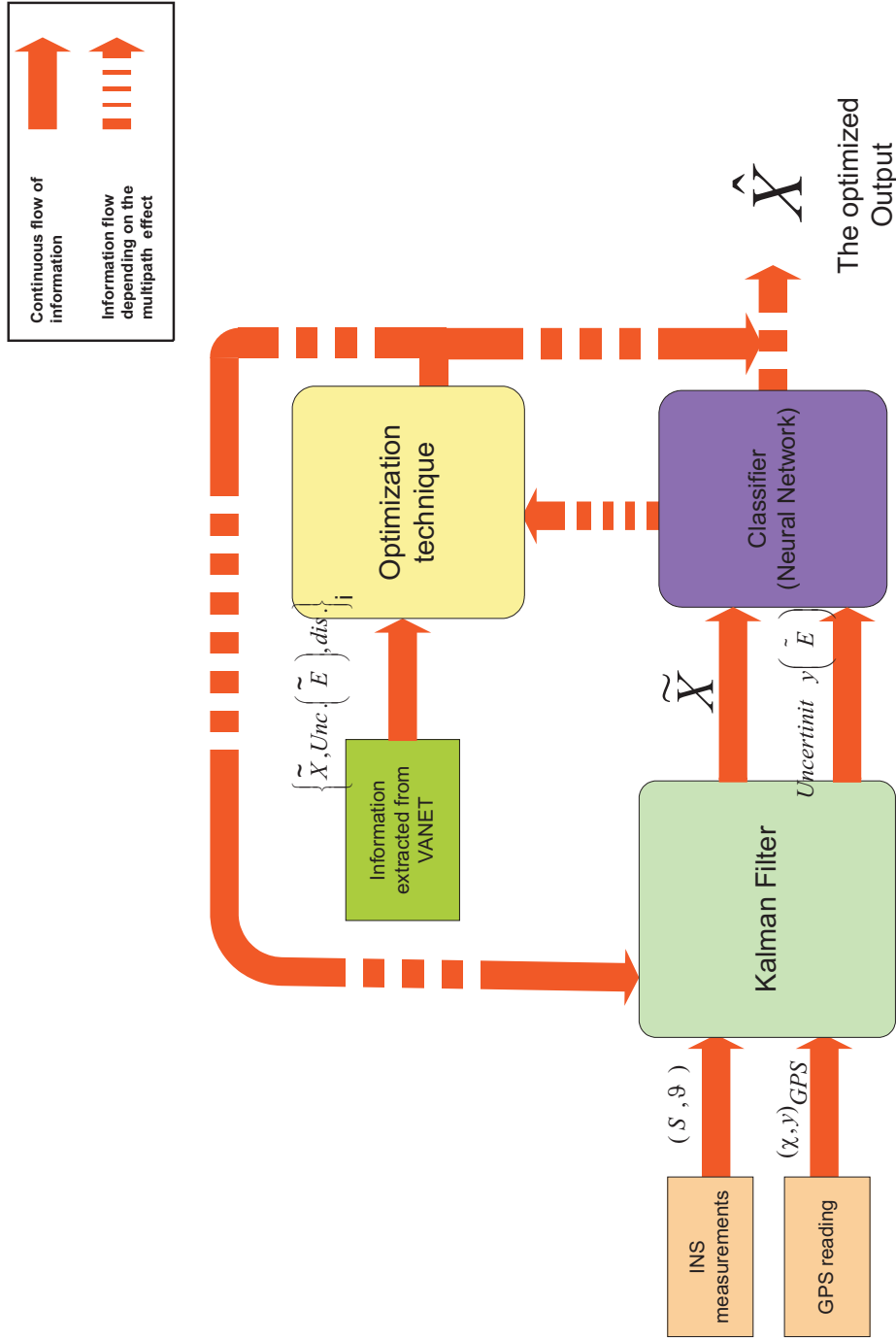


Figure 3.3: Block diagram of the proposed technique.



certain these vehicles are about their location estimate, and the neighbours' estimated locations. This information compensates for the loss of the satellite signals and corrects the errors caused by the multipath effect since not all nodes suffer from a multipath effect at the same time. Thus, at any specific time, nodes with the smallest uncertainty may be considered as anchors. These nodes can be used as reference points to help improve the estimation of the locations of their neighbours by providing distances among nodes. Similar localization methods are used in wireless sensor networks, such as PLACE in [26] or semidefinite programming optimization techniques (SDP), in [27]. The advantage that VANET has over a wireless sensor network is that the initial solution for the optimization problem is close to the optimal solution since VANET already uses GPS receivers. In addition, also the number of neighbours is smaller than in a wireless sensor network, which will expedite solving the optimization problem.

Before the details of optimizing the location estimation are discussed, the integration of GPS measurements and INS measurements using Kalman Filter is explained.

## 3.2 Kalman Filter a Location/Data Tool

A Kalman Filter has been implemented in order to improve the accuracy of the localization in different ways, such as in [7, 8, 9, 10, 11]. Without loss of generality, a fixed speed and direction model is used here, since all the experiments are simulated without any kinematic model in MATLAB. Chapter 4 provides more details. For every vehicle<sup>1</sup> that starts moving from a known location  $X_k \in \mathbb{R}^2$  at time  $t_k$ , it is possible to estimate its location after a period of time  $\Delta t$  (sampling period) as follows:

$$X_{k+1} = X_k + \Delta t \times \dot{X}_k \quad (3.1)$$

where vector  $X_k$  signifies the exact vehicle location, which will be called the state, at time  $t_k$ , and the vector  $\dot{X}_k \in \mathbb{R}^2$  signifies the vehicle velocity which obtained from the Inertial Navigation System at  $t_k$  as follows:

$$\dot{X}_k = \begin{pmatrix} \dot{x} \\ \dot{y} \end{pmatrix}_k = S_k \times \begin{pmatrix} \cos \theta_k \\ \sin \theta_k \end{pmatrix} \quad (3.2)$$

where  $S \in \mathbb{R}$  signifies the vehicle speed, and  $\theta \in [0^\circ, 360^\circ]$  signifies the vehicle direction with respect to the global axis.

---

<sup>1</sup>Note that the vehicle index is dropped because the concern here is not about a specific vehicle

In addition, every vehicle has a location measurement obtained by means of its GPS receiver, which is indicated by

$$Z_{GPS,k} = \begin{pmatrix} x \\ y \end{pmatrix}_{GPS,k} \quad (3.3)$$

where  $k \in \{0, 1, 2, \dots\}$  signifies an index of the measurement sample at  $t_k$ , and  $x, y \in \mathbb{R}$  signify the vehicle's global coordinates. A discrete Kalman Filter is used to integrate these two measurements as follows:

$$\begin{aligned} X_{k+1} &= AX_k + BU_k + w_k \\ Z_{k+1} &= HX_{k+1} + \zeta_{k+1} \end{aligned} \quad (3.4)$$

where

$$A = \begin{pmatrix} 1 & 0 \\ 0 & 1 \end{pmatrix}, B = \begin{pmatrix} \Delta t & 0 \\ 0 & \Delta t \end{pmatrix}, H = \begin{pmatrix} 1 & 0 \\ 0 & 1 \end{pmatrix}$$

where  $X_{k+1}$  is a  $2 \times 1$  vector that signifies the state or location of the vehicle at time  $t_{k+1}$ , given the location and the velocity at time  $t_k$ ;  $U_k$  is a  $2 \times 1$  vector that signifies the input of the Kalman Filter that is the INS measurement at time  $t_k$  (vehicle velocity); and  $Z_{k+1}$  is a  $2 \times 1$  vector that signifies the expected GPS

reading at  $t_{k+1}$ . The matrices  $A, B$ , and  $H$  are  $2 \times 2$  transition matrices that relate the current state and current input to the next state, and the expected state to the next GPS measurement, respectively. It is also assumed that  $w_k$  and  $\zeta_k$  are  $2 \times 1$  vectors that signify random variables that represent the process and the measurement noise. They are assumed to be independent and white with a normal probability distribution:

$$P(w) \sim N(0, \mathbf{Q})$$

$$P(\zeta) \sim N(0, \mathbf{R})$$

$\mathbf{Q}$  and  $\mathbf{R}$  are  $2 \times 2$  matrices that signify the process noise covariance and the measurement noise covariance, respectively.  $\mathbf{Q}$  and  $\mathbf{R}$  may change over time in the real world. These two matrices resemble the covariance of the INS error and the error of the GPS receiver when no multipath effect is present. Thus, it is assumed that they are constant.

Practically, it is impossible to separate these two types of noise from the measurements, so the system in Equation (3.4) is implemented as follows:

$$\begin{aligned} X_{k+1/k} &= AX_{k/k} + BU_k \\ Z_{k+1/k} &= HX_{k+1/k} \end{aligned} \tag{3.5}$$

where  $X_{k+1/k}$  is defined as an a priori state estimate and  $X_{k/k}$  is defined as an a posteriori state estimate, which can be calculated given the GPS measurement at  $t_k$  as shown below. Accordingly, two types of estimation errors are introduced: an

apriori estimate error  $2 \times 1$   $e_{k+1/k}$  and an aposteriori estimate error  $2 \times 1$   $e_{k+1/k+1}$ :

$$\begin{aligned} e_{k+1/k} &= X_{k+1} - X_{k+1/k}, \text{ and} \\ e_{k+1/k+1} &= X_{k+1} - X_{k+1/k+1}. \end{aligned} \tag{3.6}$$

The apriori estimate error covariance is then

$$P_{k+1/k} = E [e_{k+1/k} e_{k+1/k}^T], \tag{3.7}$$

and the aposteriori error estimate is

$$P_{k+1/k+1} = E [e_{k+1/k+1} e_{k+1/k+1}^T] \tag{3.8}$$

The goal of the Kalman Filter is to compute an aposteriori estimated state  $X_{k+1/k+1}$  using an apriori estimated state  $X_{k+1/k}$  and a weighted difference between an actual measurement  $Z_{k+1}$  and an estimated measurement  $Z_{k+1/k}$ , as shown below:

$$\begin{aligned} X_{k+1/k+1} &= X_{k+1/k} + G (Z_{k+1} - Z_{k+1/k}) \\ &= X_{k+1/k} + G (Z_{k+1} - H X_{k+1/k}). \end{aligned} \tag{3.9}$$

A difference of zero between the predicted measurement and the actual measurement means that the two are in complete agreement. This difference is called the residual. The residual reflects the discrepancy between the estimated and the actual measurement.

The matrix  $2 \times 2$   $G$  in Equation (3.9) is chosen to be a blending factor that minimizes the aposteriori estimate error covariance in Equation (3.8). This minimization can

be accomplished if Equation (3.9) is substituted in (3.6), the expectation of Equation (3.8) is performed, the derivative of the trace of the result with respect to  $G$  is taken, and  $G$  is solved for after the result is set to equal zero. More details are included in Appendix A.  $G$  has different forms, one of which is the following:

$$G_{k+1} = P_{k+1/k} H^T (H P_{k+1/k} H^T + \mathbf{R})^{-1}. \quad (3.10)$$

This blending factor is called the Kalman gain. In addition, the apriori and aposteriori error covariance can be defined as

$$P_{k+1/k} = A P_{k/k} A^T + \mathbf{Q} \quad (3.11)$$

$$P_{k+1/k+1} = (I - G_{k+1} H) P_{k+1/k}. \quad (3.12)$$

With the above equations, all the quantities required for estimating the system state at  $t_{k+1}$  are determined. Equations (3.5), (3.9), (3.10), (3.11), and (3.12) comprise the Kalman Filter recursive equations. Figure 3.4 shows a block diagram depicting the discrete Kalman Filter loop that is used to estimate the system's next state in every cycle with the optimal error reduction. Two basic stages are described in Figure 3.4: the Time Update stage and the Measurement Update stage. In the first, the INS measurement is obtained and used to estimate the next location after  $\Delta t$  and to calculate the apriori error covariance matrix  $P_{k+1/k}$ . In the second, the GPS receiver measurement is obtained and fused with the result of the Time Update stage after calculating the Kalman Filter gain  $G$ . The aposteriori error covariance

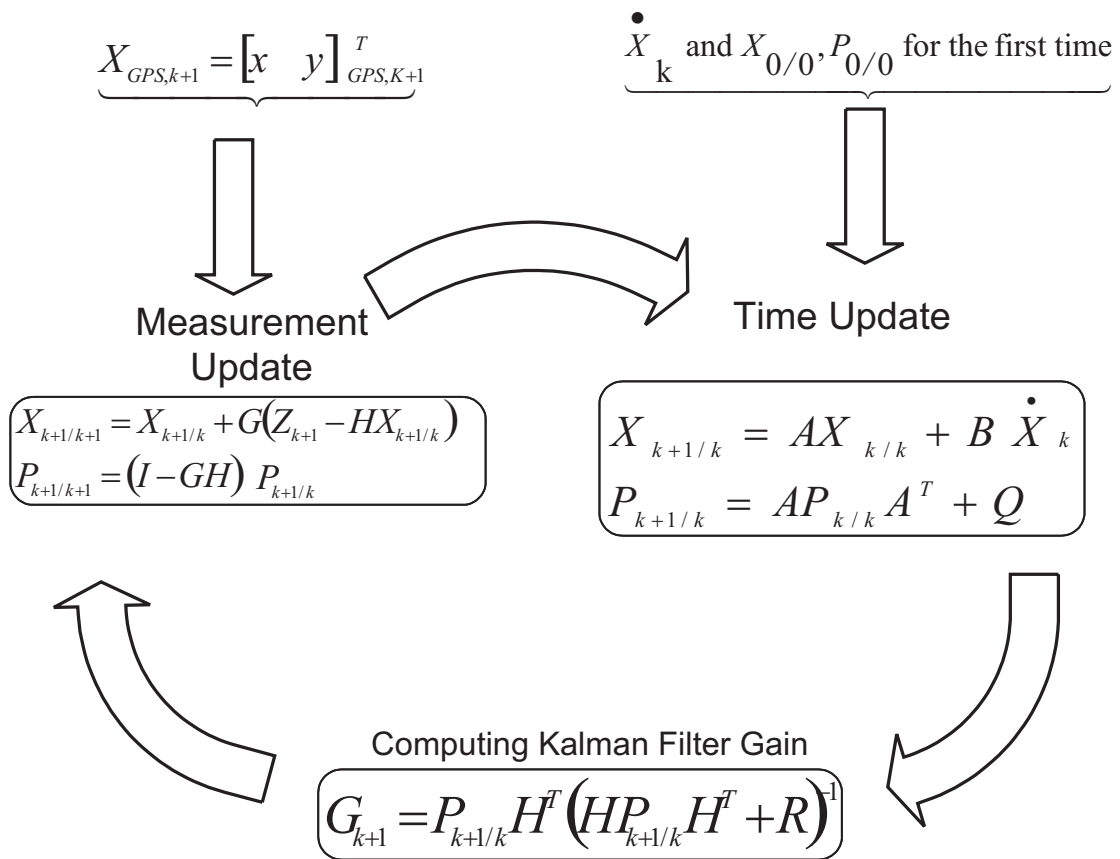


Figure 3.4: The discrete Kalman Filter loop.

is also calculated in the Measurement Update stage because, it is needed in order to provide the filter with the initial state or location  $X_{0/0}$  and the initial covariance error  $P_{0/0}$ , which will start the filter.

### 3.3 Improving Localization in a Multipath Environment

Although the Kalman Filter estimates locations with a minimum mean square error, which is an optimum estimate [28], in many cases, it produces unexpected errors as a result of multipath effects or the loss of the satellite signals. The focus in this thesis is on minimizing the multipath effect. However, reducing the multipath effect is only one aspect of the problem; detecting the multipath effect is another challenge. The proposed technique works in conjunction with the Kalman Filter to help vehicles detect the presence of the multipath effect in their location estimates. The multipath effect adds noise to the location estimate and contaminates the randomness of the measurement error so that it can not be represented by the matrix  $\mathbf{R}$  of the Kalman Filter. Accordingly, the Kalman Filter is not optimum in cycles when the multipath effect is present. In such cases to overcome this problem, the vehicle should communicate with its neighbours in VANET, which is not affected or is less affected by the multipath disturbance. However, this strategy is not always reliable because any target vehicle will find many neighbours that suffer from the same problem. These neighbours might mislead the target vehicle in its estimation of the location. Thus, it is important to find a measurement that can tell how accurate these neighbours are. This measurement will help select the best three



neighbours and will consider them to be anchors<sup>2</sup>, which can be used to localize the target vehicle more accurately.

The following subsections explain the vehicles' evaluation of uncertainty, the use of Neural Networks (NNET) for detecting the multipath effect, and the use of the Least Square (LS) optimization method to improve the estimate of the location.

### **3.3.1 Evaluation of Uncertainty in Localization**

Uncertainty in the estimation of a location is a measurement of how much any vehicle is uncertain about its location estimate. When it is communicating with its neighbours to look for more accurate localized vehicles to use as reference nodes, this measurement helps a target node. With the proposed technique, every vehicle must be aware of the uncertainty of the location estimate because it prevents vehicles with unreliable information from misleading other vehicles. Thus, all vehicles should update their uncertainty measurement after every cycle of the Kalman Filter estimation, and should associate the Kalman Filter location estimate with this measurement. These two pieces of information are sent by the neighbours of a target vehicle when it asks for a correction in the location estimation. The target

---

<sup>2</sup>In this thesis, the localization is considered to be in two dimensions; if three dimensions is required for localization, then the minimum number of anchors is four.

node compares the neighbours' uncertainty measures and selects the best three to use as anchors.

In this thesis, the uncertainty of a vehicle's location is represented by the variation in the discrepancy between the time update estimate of the Kalman Filter and the GPS receiver measurement as follows (from Equation 3.9):

$$Discrepancy = Z_{k+1} - HX_{k+1/k}$$

multipath effect in the GPS receiver measurement will be reflected in the discrepancy value. Every vehicle should record the number of previous discrepancy values. The number of these values should be neither too small nor too large in order to well represent the uncertainty of the recent location estimation.

When a vehicle does not experience any multipath effect, the accuracy of the GPS accuracy will be good and the discrepancy values will be small and almost identical. As a result, the variation in the discrepancy values will also be small. In other words, this vehicle will have a small uncertainty about the location and it can therefore be used as a reference node for its neighbours.

However, if a vehicle experiences a multipath effect, the accuracy of the GPS will

be drastically affected and the discrepancy values will be totally and randomly different. As a result, the variation in the discrepancy values will be large. In other words, this vehicle will have a large uncertainty about the location, and it should not be used as a reference node for its neighbours in order to avoid misleading them.

Often after experiencing a multipath effect, the Kalman Filter needs time to converge to the right estimation. Since every vehicle stores the previous discrepancy values, the uncertainty of the location estimate will remain large for a while even after a vehicle leaves the multipath region. This large uncertainty prohibits the use of this vehicle as a reference node, thus saving its neighbours from the non-converged Kalman Filter estimation.

In Equation 3.9, the discrepancy between the estimated location in the first stage and the actual measurement reflects the divergence between the GPS receiver's measurement and the location estimate. This divergence can be used as a pattern to show whether a multipath effect is present. Taking different GPS measurements that include some multipath effects and training the neural network using these divergence patterns in a supervised learning manner produces a classifier that can look at new divergence patterns and classify them as multipath-affected measurements or not.

### 3.3.2 Detection of the Multipath Effect Using NNET

A neural network is an artificial intelligence method that models the human brain. A neural network can be trained to classify different patterns that belong to known classes via supervised or unsupervised learning methods. It often consists of a number of layers and nodes, as shown in Figure 3.5 in which the information flows from the nodes in one layer to other nodes in the following layer until the information reaches the output layer, which is responsible for making decisions.

The type of neural network that has been chosen in this study is a Feed-Forward Backpropagation Network since it falls under the supervised learning category of Artificial Neural Networks (ANN). It is also easy to construct and implement in MATLAB. It has been constructed to form three layers (input, hidden, and output) as shown in Figure 3.6. This construction simplifies and accelerates the training procedure. The number of neurons (i.e., nodes) in the input and hidden layers may seem a bit high (between 30 and 50) in order to achieve good representation for the input range. Hyperbolic tangent sigmoid transfer functions have been used in the neurons of the input and hidden layers. The output layer is comprised of one neuron, which provides a weighted linear combination of the output of the hidden neurons.

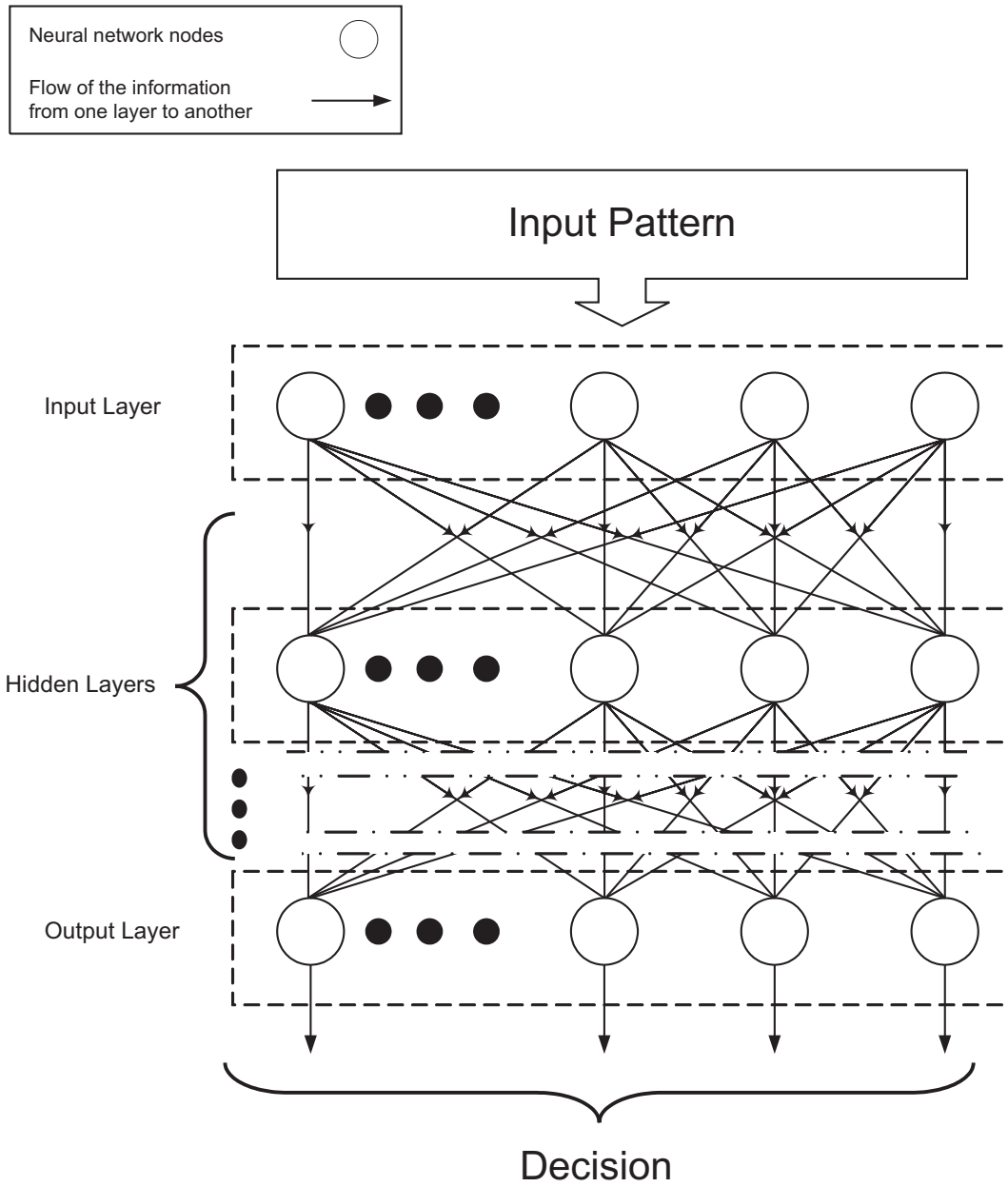


Figure 3.5: Architecture of a general neural network.

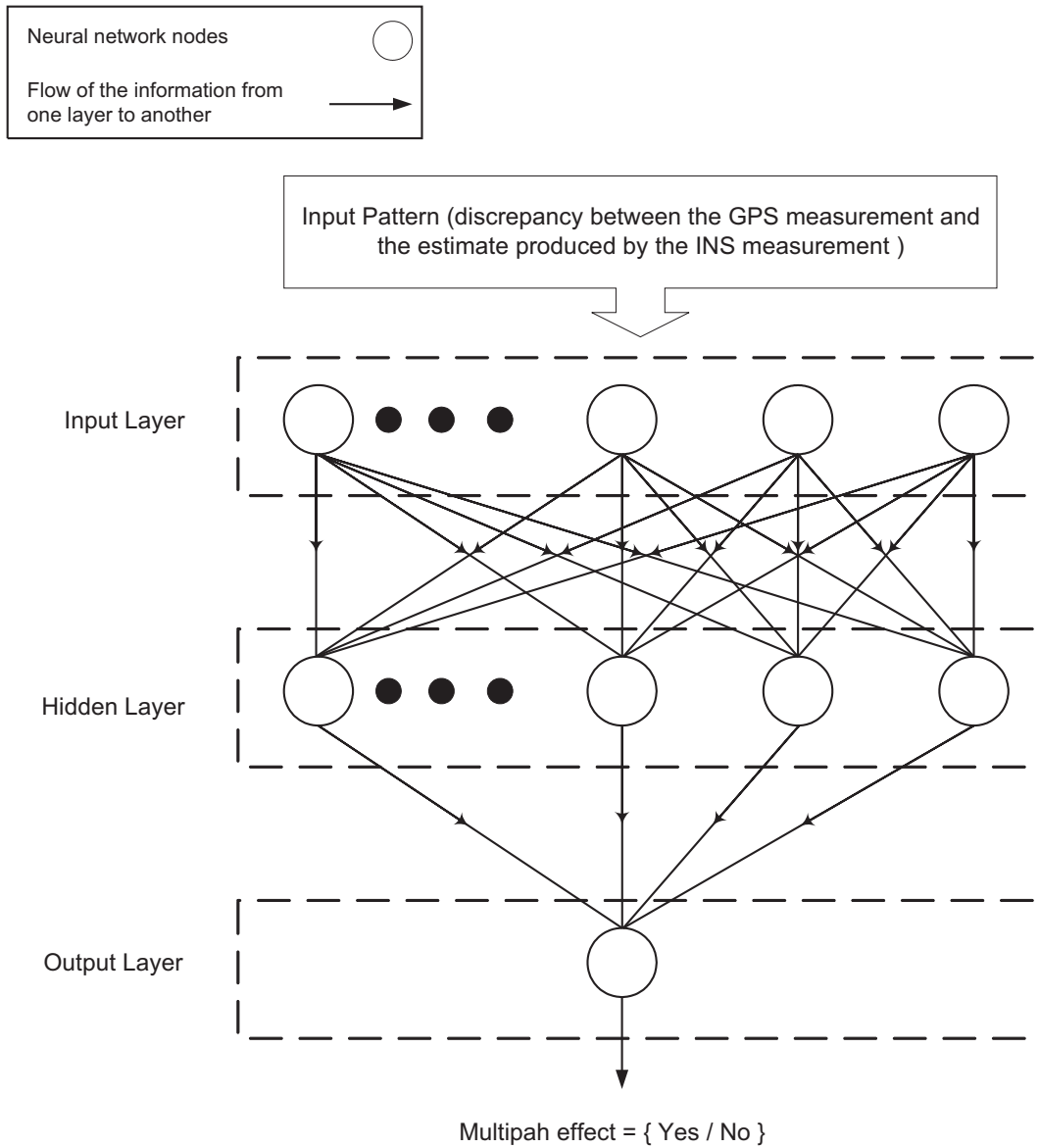


Figure 3.6: Neural network for detecting the multipath effect.

### 3.3.3 An Algorithm for Improving the Location Estimate

When a vehicle detects that its location estimate has been contaminated by the multipath effect, the following algorithm must be performed in order to minimize the impact of the multipath effect:

1. The target vehicle ( $V_o$ ) sends a message to its neighbours announcing that its location estimate needs to be corrected.
2. The target vehicle's neighbours ( $V_1, V_2, V_3, \dots, V_n$ ) reply by sending their location estimates and their uncertainty evaluations.
3. The distances ( $d_{0,1}, d_{0,2}, \dots, d_{0,n}$ ) between the target vehicle  $V_o$  and every neighbour (i.e.,  $V_1$  to  $V_n$ ) are determined using one of the techniques mentioned in [21].
4. The target vehicle chooses as reference nodes three neighbours that, according to their uncertainty evaluation, have much better accuracy<sup>3</sup> than the target vehicle.
5. If there are enough more accurate vehicles (three reference nodes), the target vehicle corrects its location estimate using the Least Square formulation, which is described later in this section.

---

<sup>3</sup>A fraction of the target vehicle's uncertainty is set as a threshold and the uncertainty of every neighbour is compared to this value.

6. If there are not enough accurate vehicles (less than three reference nodes), then the contaminated Kalman Filter estimation is replaced by the time update estimate of the Kalman Filter.
7. The corrected location estimate is fed back to the Kalman Filter.
8. The uncertainty of the target vehicle is updated. If there are enough reference nodes, the worst uncertainty measurement among them is used; if not, the contaminated uncertainty measurement is just omitted.

Step 6 takes advantage of the small error caused by the INS system over a short time and cancels the contaminated location estimate. The likelihood of not having enough anchors is remote because not all the vehicles suffer from the multipath effect simultaneously. In addition, the surrounding environment different from one vehicle to another and changes quickly with the vehicle's movement. However, even if this situation occurs, it will not last for long, which guarantees that the location estimate will not be negatively affected using INS measurements. Figure 3.7 shows the flow chart of the algorithm, and sections 3.3.4 and 3.3.5 describe two of its components.



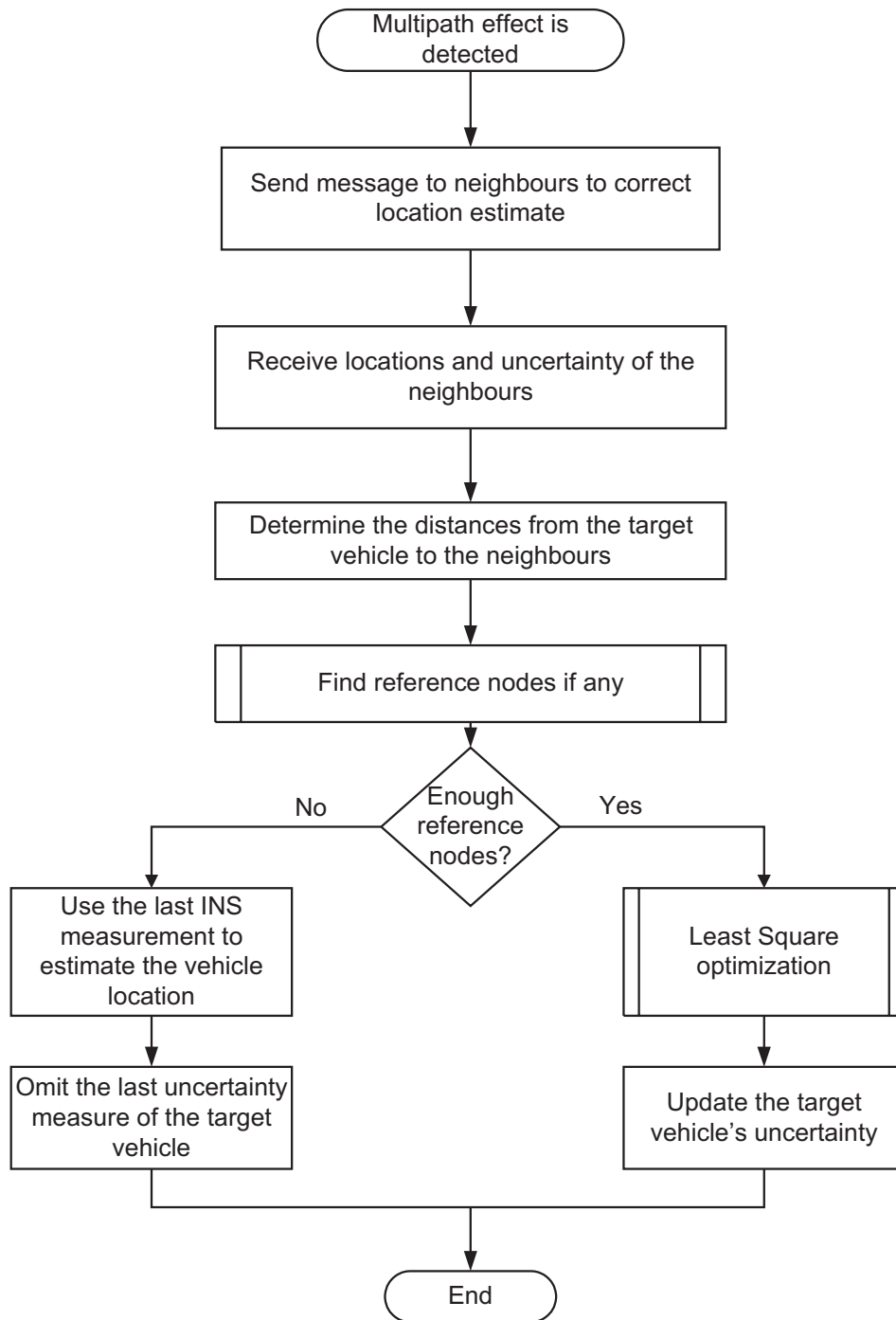


Figure 3.7: The flowchart of the algorithm for improving the location estimate.

### 3.3.4 The Least Square Minimization of the Localization Error

If the target vehicle is able to find three reference nodes, it corrects its location estimate using the least square formulation, as follows.

Let  $\tilde{X}_0$  be the target vehicle location estimate that the Kalman Filter computed at time  $t_k$ .  $X_a$ ,  $X_b$ , and  $X_c$  are the locations of the three vehicles that have the most accurate location estimate in the vicinity of the target vehicle  $V_o$ . Let  $a, b, \&c \in 1, 2, 3, \dots, n$ , where  $a \neq b \neq c$ . At time  $t_k$ , the classifier detects a multipath effect, so the target location can be optimized according to the following optimization problem:

$$\hat{X}_0 = \underset{\tilde{X}_0}{arg \min} \sum_{i \in I} \left( d_{0,i} - \|\tilde{X}_0 - X_i\| \right)^2 \quad (3.13)$$

where

$I = \{a, b, c\}$  is the index set of the selected anchors,

$X_i$  are the locations of the selected anchors,

$d_{0,i}$  is the distance between the target node  $V_0$  and the anchor  $V_i$ ,

$\hat{X}_0$  is the optimized location estimate, and

$\tilde{X}_o$  is the initial location of the target vehicle  $V_o$ .

The above optimization problem is nonlinear, continuous, and convex. It can therefore be solved with the Nelder-Mead method. This method can be implemented without calculating the gradient vector or the Hessian matrix, which makes it very efficient. Next, we will describe Nelder-Mead method for solving derivative-free

optimization problem.

### 3.3.5 The Nelder-Mead Method of Optimization

The Nelder-Mead method is also called the simplex-reflection method, which takes its name from the fact that the concern is always about  $n + 1$  points in a space  $\mathbb{R}^n$ , whose convex hull forms a simplex [29]. If  $\mathcal{S}$  is a simplex that has vertices  $\{z_1, z_2, \dots, z_{n+1}\}$ , then in a single iteration of this method, a function, such as Equation 3.13, is evaluated at every vertex and an attempt is made to replace the vertex that has the worst value with a vertex that has a better function value. The new point is determined by reflecting, expanding, or contracting the simplex along the line joining the worst vertex and the centroid of the remaining vertices. If there is no better point, the simplex is shrunk by retaining the vertex with the best value and moving the other vertices toward this vertex. To start the method, the vertices are ordered according to their function values, as follows:

$$f(z_1) \leq f(z_2) \leq \dots \leq f(z_{n+1})$$

The centroid of the best  $n$  points is defined by

$$\bar{z} = 1/n \sum_{i=1}^n z_i,$$

and the points along the joining line between the centroid and the worst vertex  $z_{n+1}$  are defined as

$$z(t) = \bar{z} + t(z_{n+1} - \bar{z})$$

where  $t$  is a scalar used to perform contraction and expansion via assigning values, such as  $-1$ ,  $-2$ ,  $-\frac{1}{2}$ , and  $\frac{1}{2}$ .

The Figure 3.8 shows the flow chart of one step of the Nelder-Mead optimization method in which the new candidate points are examined in order to replace them with the vertex  $z_{n+1}$ , or to shrink the simplex toward the best vertex  $z_1$  and start the next step. This process is repeated until the optimal vertex is reached.

In Figure 3.9, an example of three-dimensional space  $\mathbb{R}^3$ , which is the case in this thesis, is used to illustrate the flow chart. In Figure 3.9, the worst vertex is  $z_3$ , and the possible new candidate points are  $\bar{z}(-1)$ ,  $\bar{z}(-2)$ ,  $\bar{z}(-\frac{1}{2})$ , and  $\bar{z}(\frac{1}{2})$ . If none of the new candidates proves to be satisfactory, the simplex will be shrunk toward  $z_1$  as depicted by the dashed line. It can be noted that the new simplex will retain the best vertex  $z_1$ .

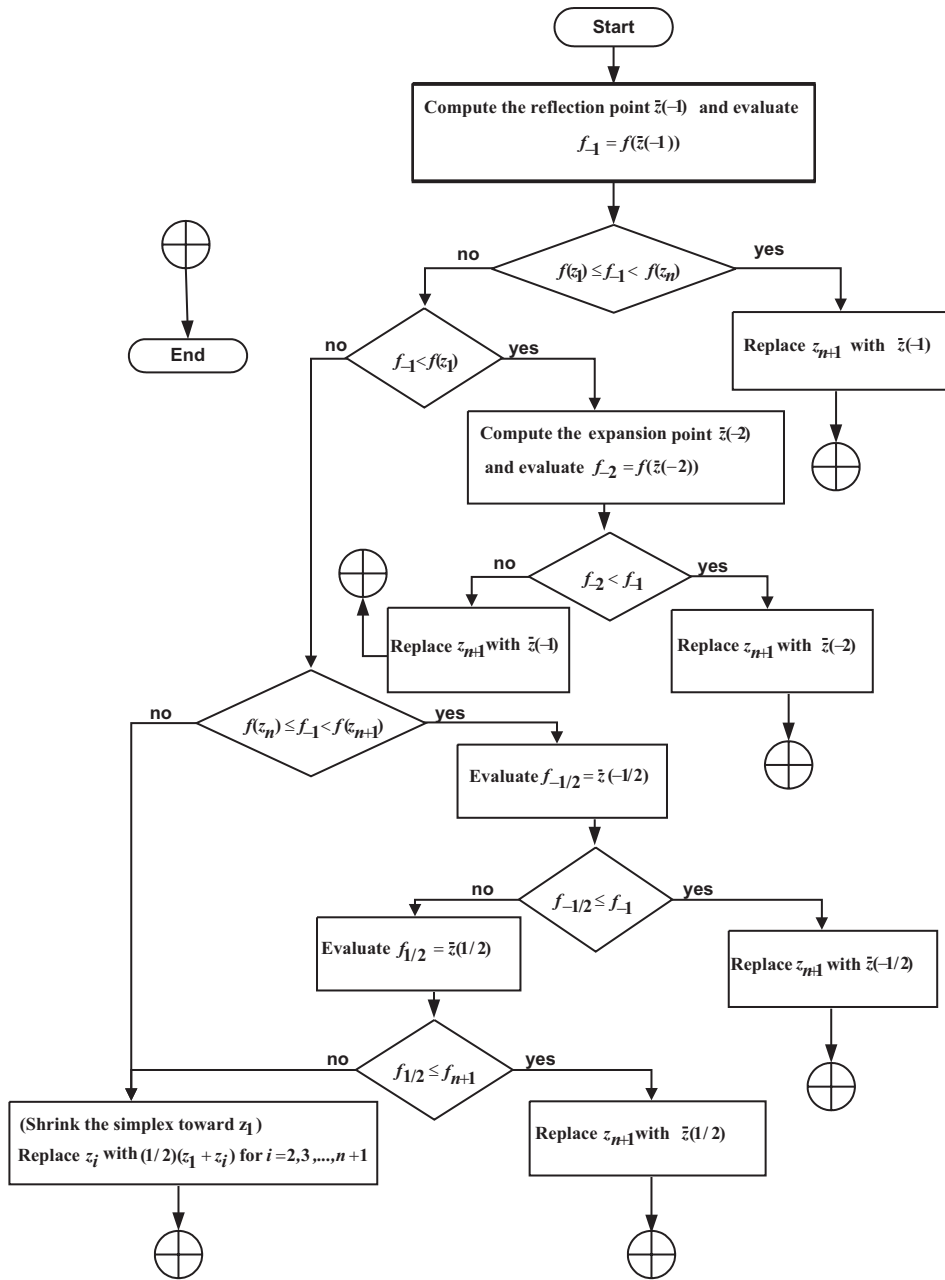


Figure 3.8: The flow chart of the Nelder-Mead optimization method.

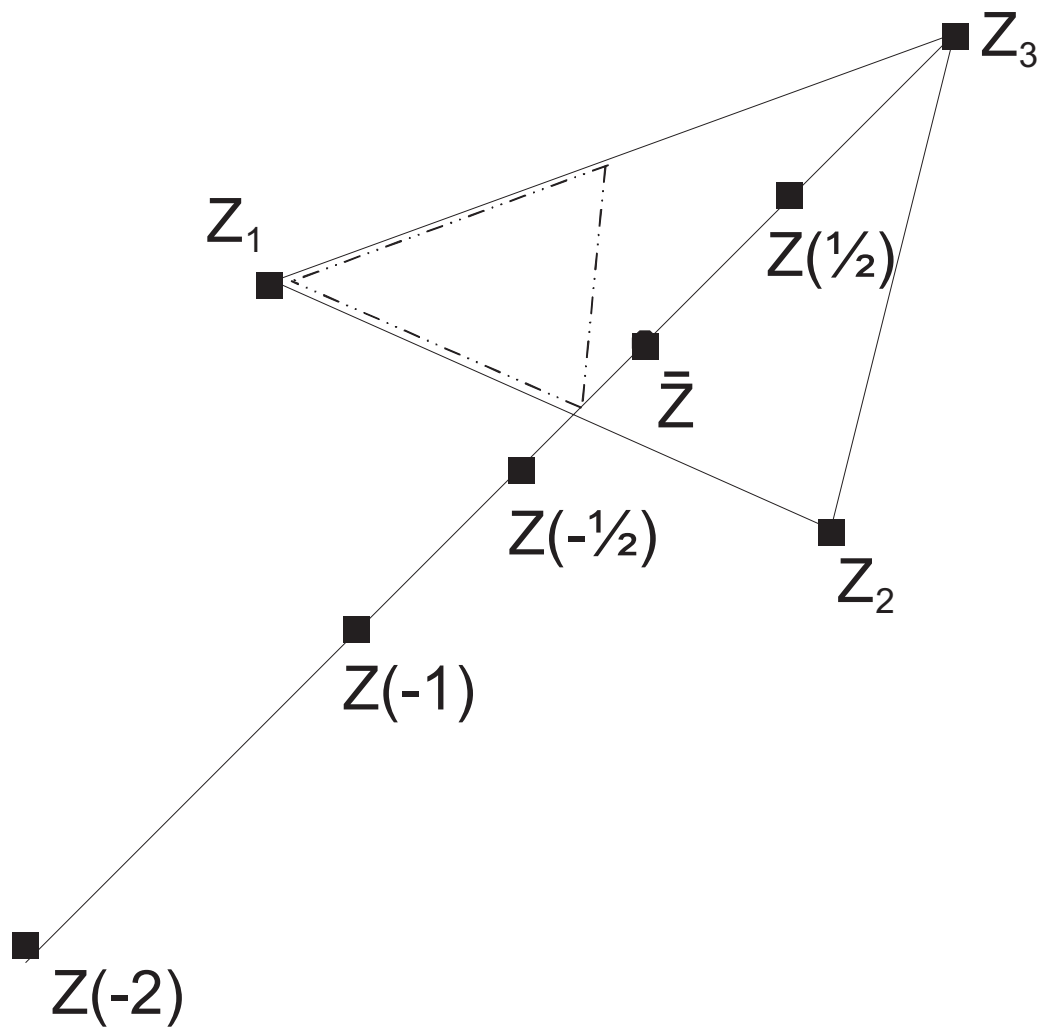


Figure 3.9: One step of the Nelder-Mead simplex method in  $\mathbb{R}^3$ .

## 3.4 Summary

This chapter illustrates how the Kalman Filter can be used to integrate the GPS satellite receiver readings and the INS measurements. However, this integration can not avoid the misleading results of the multipath effect, which becomes severe in regions with many rise buildings, trees, or tunnels.

In the proposed technique, an artificial neural network is fist used to detect the multipath effect. Next, the target vehicle selects the most accurate vehicles from its neighbours and uses them as reference points to correct its location estimate via an optimization technique. The target vehicle then updates its uncertainty measurement according to the way in which it corrected its location estimate.

Chapter 4 presents experimental work to validate and analyze the results of the experiments, and the analysis of the results of modifying parameters that affect performance.

# Chapter 4

## Experimental Results

This chapter presents the implementation of the algorithms and theoretical work explored in Chapter 3. First, the implementation of the Kalman Filter for a single vehicle is described. then, the effect of multipath signals on GPS readings and the performance of the Kalman Filter are demonstrated. Next, the plan of the simulation scenarios and the experimental steps for a group of vehicles in VANET are explained. The chapter concludes with a discussion of the results and a comparison of the different cases and scenarios.

Since performing a real-time experiment in VANET is somewhat expensive, all experiments are simulated using MATLAB. The main purpose of the simulation is to show the improvement the IVCALS technique produces in the accuracy of the location estimate for a vehicle that is equipped with a normal GPS satellite receiver.



Neither the routing protocols nor the Medium Access Control (MAC) protocols are discussed in this thesis because the communication service that is needed in the IV-CALS technique requires communication only among neighbours that are no more than one hop away. In addition, the amount of the data exchanged is not large, and can be encapsulated in small packets that will minimize the contention in the MAC layer.

## 4.1 Setup Kalman Filter Implementation

The problem with estimating location as discussed in this thesis is fundamentally caused by local and global GPS receiver errors as well as the INS measurement error, as explained in Chapter 2. According to Equation (3.2), If there is any error in the INS measurements, the vehicle's speed or direction; the system state will be affected. In a Kalman Filter, the error in the state is represented by the process noise covariance matrix

$$\mathbf{Q} = \sigma_Q^2 I$$

Based on the research that has tackled the modeling and analysing of such errors [24, 25],  $\sigma_Q$  was set to 0.5 *m*. The local and global errors in the GPS receiver are represented by the measurement noise covariance matrix of the Kalman Filter

$$\mathbf{R} = \sigma_R^2 I,$$

where  $\sigma_R$  is set to be between 10 and 15 m, which is approximately the variance in the total GPS receiver error in an open area. However,  $\mathbf{R}$  does not represent the measurement error covariance matrix when the Kalman Filter estimation has deteriorated because of the multipath effect. In such cases, the variance in the GPS receiver reading becomes between 100 and 150 m, and this random change results in a dramatic increase in the uncertainty in the Kalman Filter estimate. In the simulation, the sampling rate of the GPS receiver reading is 1 *Hz*, which is the highest frequency for any GPS receiver. In each second, the Kalman Filter can obtain one or more measurements of the INS system in order to estimate the next location via its time update stage; however, one INS measurement per second is used in the simulation because all the vehicles are moving in one direction at fixed speeds.

For example, Figure 4.1 shows how the Kalman Filter estimates the locations of a vehicle travelling over 5 km at a speed of 50 km/h. Figure 4.2 depicts the multipath effect on the same vehicle when it passes through a 500 m region containing high buildings. This region is located between the 2000 m and 2500 m points of the total distance travelled. Figure 4.3 is an enlarged part of Figure 4.2, in which it can be seen that the multipath effect is still present even after the vehicle has passed the multipath region because the Kalman Filter needs time to converge to the right

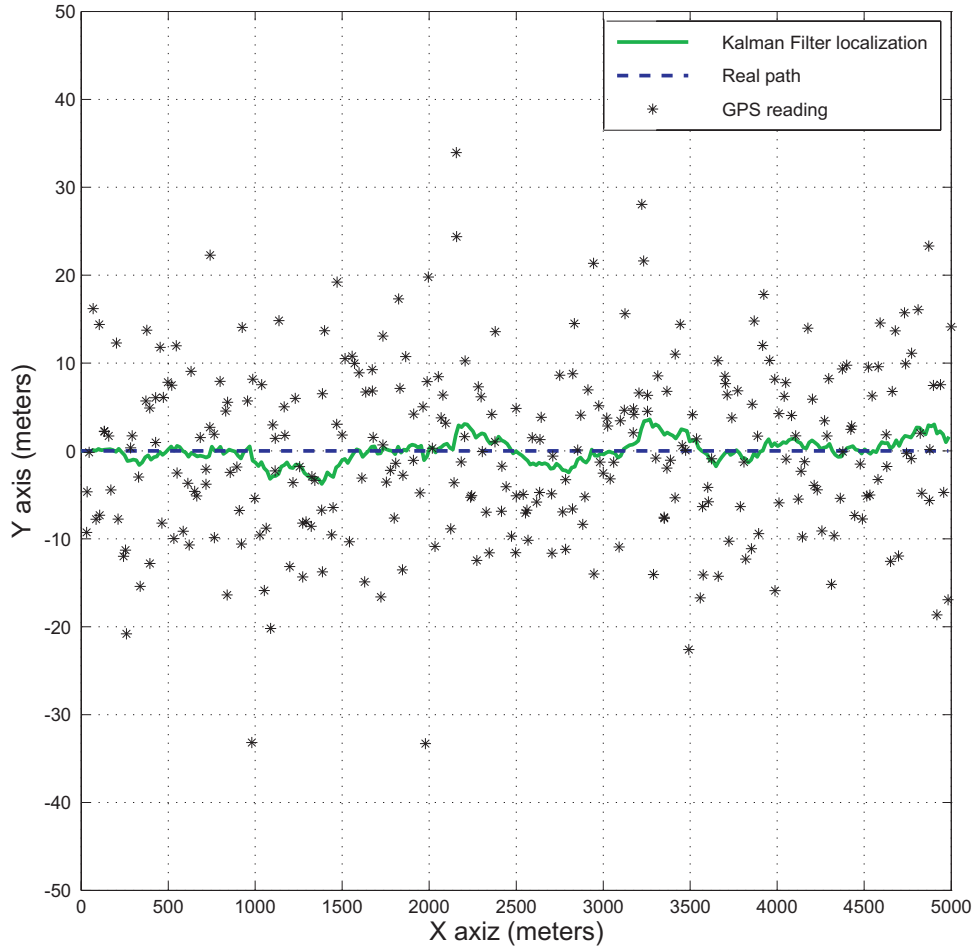


Figure 4.1: Example of the localization technique using the Kalman Filter to integrate the INS measurements and the GPS receiver readings in an open area, when  $\sigma_R = 10 \text{ m}$ .

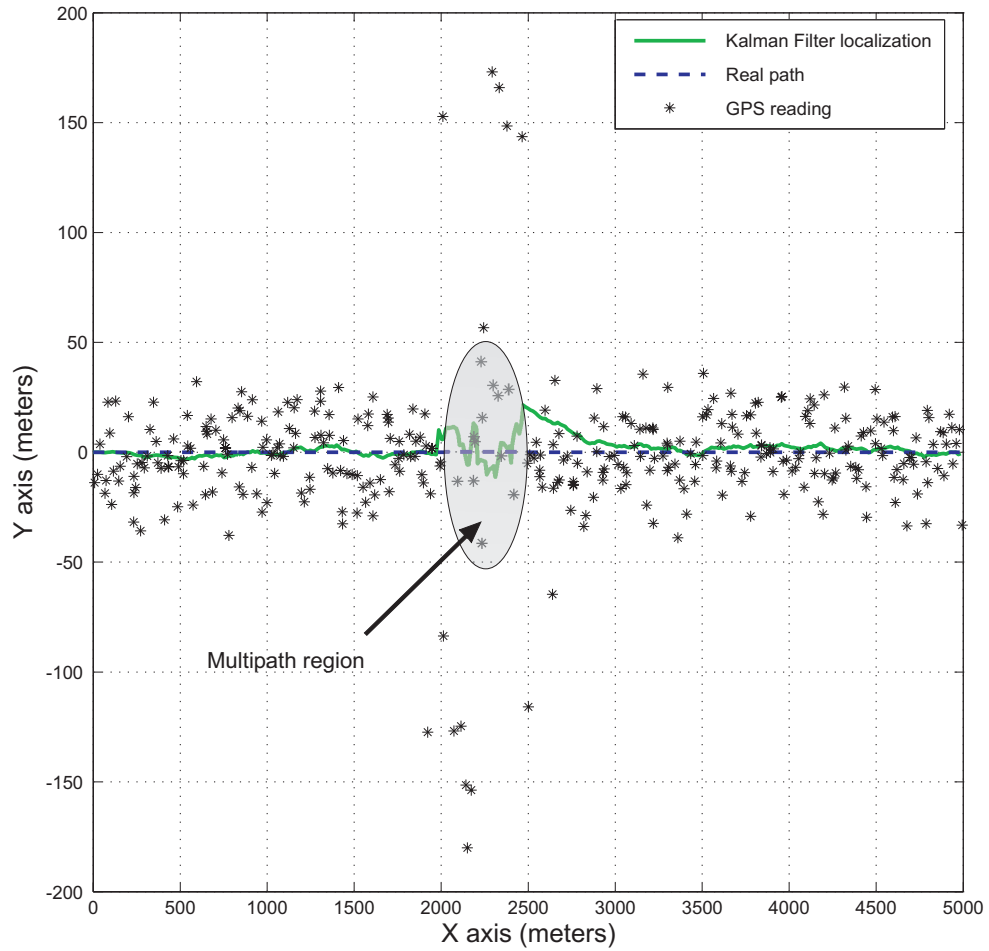


Figure 4.2: Example of the localization technique using the Kalman Filter to integrate the INS measurements and the GPS receiver reading. The vehicle in this example experience a multipath effect in an open area for 500 m, in which  $\sigma_R = 15\text{ m}$ .

location.

## 4.2 Simulation Scenario

As mentioned, the simulation for this thesis was implemented using MATLAB7. The scenario covers a 5000 m (5 km) portion of a straight road. Vehicles travelling this road experience different local environments, such as an open area with no multipath effect, and an inner-city area where high buildings cause a severe multipath effect. The road consists of two lanes in one direction for vehicles with different speeds. The right lane contains the vehicles travelling at 50 km/h, and vehicles in the left lane are travelling at a higher speed of 60 km/h. The width of each lane is 3 meters, and vehicles are assumed to be driven in the center of the lanes. The simulation uses 100 vehicles to comprise VANET. The simulation period is equal to the time required for a vehicle to pass through 5 km at a speed of 50 km/h: 360 seconds.

As shown in Figure 4.4, on the first 2000 meters of the road the vehicles travel through an open-area environment. They then experience a multipath effect over a distance of 300 meters. Another region of open area follows for 400 meters. The second multipath area occurs for the next 400 meters. Then the vehicles travel through an open area to the end of the road.

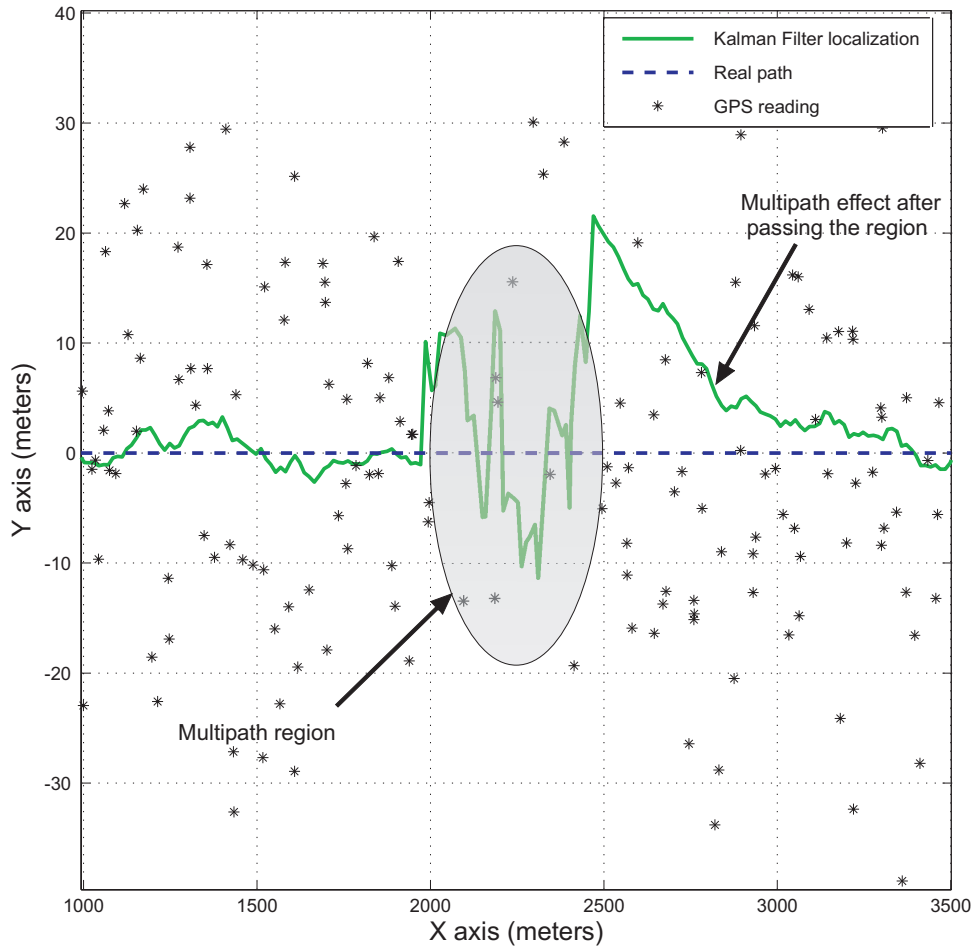


Figure 4.3: Example showing that the Kalman Filter is still influenced by the multipath effect even after the vehicle has passed the multipath region.

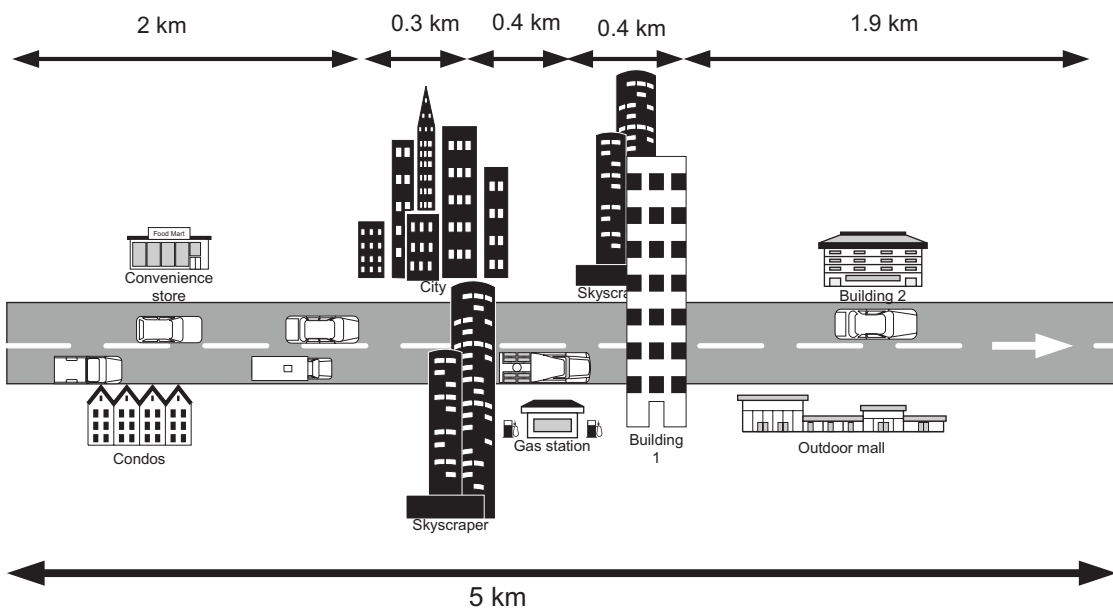


Figure 4.4: VANET simulation scenario.

To maintain the connectivity of the VANET, the number of vehicles on the 5 km is kept constant at 100. When a vehicle passes the 5 km point, a new vehicle enters the road from the opposite side.

The purpose of setting up the scenario in this way is to show the multipath effect and how long it will last after the vehicle has passed through the multipath area.

### **4.3 Results**

In the first experiment, the simulation was run without the IVCALS technique. The coordinates of a vehicle are captured while it travels over the 5 km. The vehicle's localization technique is based on integrating the INS measurements and the GPS receiver measurements via the Kalman Filter. Figure 4.5 shows how the estimate of the vehicle's location is drastically affected and becomes unreliable when the vehicle passes through high-building regions. In Figure 4.5, the dotted line represents the real path of the vehicle. The solid line represents the location estimate using the Kalman Filter.



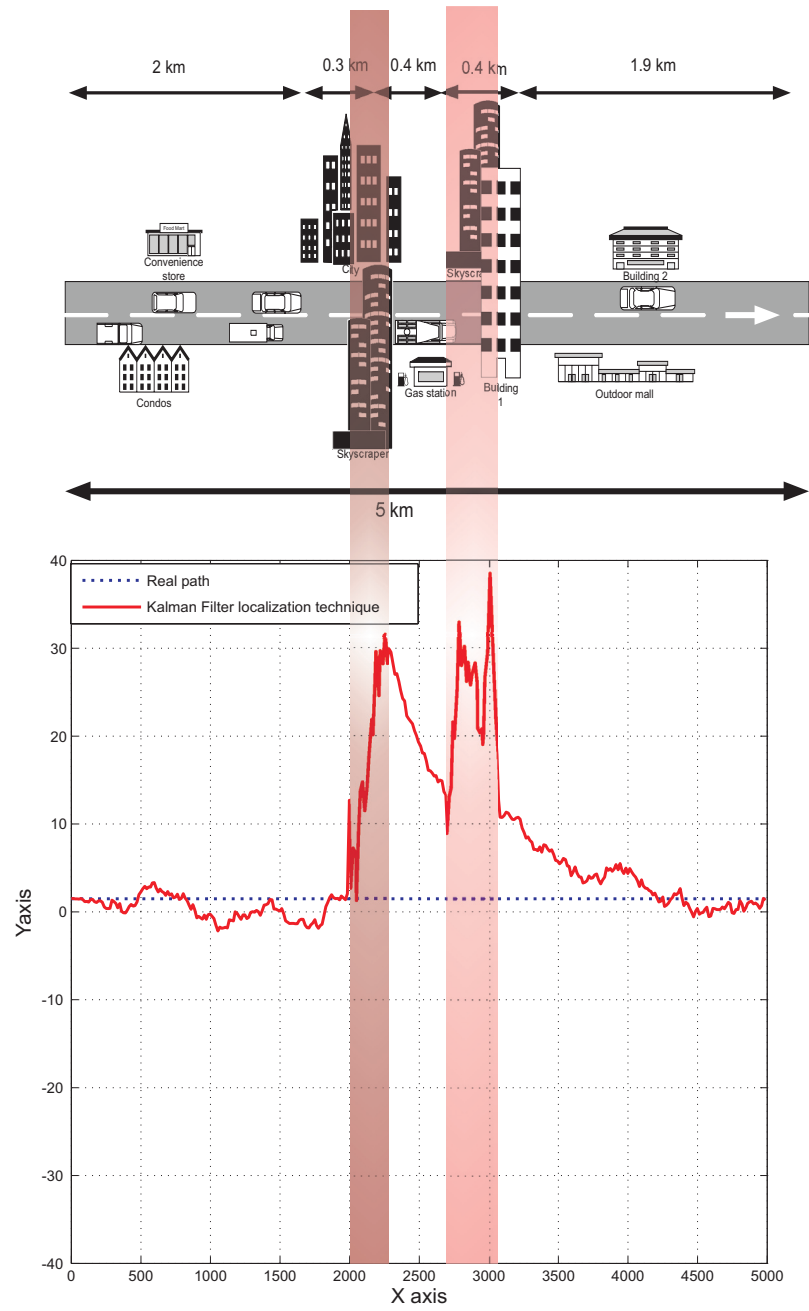


Figure 4.5: Location estimate for one vehicle in the VANET scenario, the localization is implemented using only the Kalman Filter technique.

Table 4.1: Error statistics for the localization using the Kalman Filter.

| Environment      | Distance (m) | Mean Error (m) | SD of the Error (m) |
|------------------|--------------|----------------|---------------------|
| Open area 1      | 2000         | 2.33           | 1.35                |
| High buildings 1 | 300          | 18.48          | 9.86                |
| Open area 2      | 400          | 19.43          | 5.13                |
| High buildings 2 | 400          | 24.01          | 7.11                |
| Open area 3      | 1900         | 4.92           | 4.50                |

The statistics related to the localization error are provided in Table 4.1. These statistics are calculated by computing the localization error  $LE_t$  in every second ( $t$ ), since the localization technique estimates locations every second. Then the mean and the standard deviation of the localization errors are computed for different distances according to the local environments.

$$LE_t = \|X_{real}^t - \hat{X}^t\|_2$$

$$Mean\ Error = \frac{1}{N} \sum_{t=t_1}^{t_2} LE_t$$

$$Standard\ Deviation\ of\ the\ Error = \left( \frac{1}{N} \sum_{t=t_1}^{t_2} (LE_t - MeanError)^2 \right)^{1/2}$$

where  $t_1, t_2$  signify the times of entering and leaving a region, and  $N$  signifies the number of samples in a region.

In table 4.1, the first column shows the type of environment that the vehicle expe-

riences, the second column lists the length of the distance traversed in that environment, and the third and fourth columns give the mean error and the standard deviation of the error in location estimate, respectively. It can be seen that the localization technique using the Kalman Filter can be reliable in the first open-area region. However, the increase in the standard deviation and the mean of the localization error in the first high-building region proves the unreliability of the location estimation technique using the Kalman Filter in the presence of the multipath effect. Moreover, the multipath effect still appears in the mean and the standard deviation of the localization error during the second open area region even after the vehicle has left the first high-building region. In the second high-building region, the mean of the localization error dramatically increases because the localization error has been large since the beginning of this region. The multipath effect remaining in the location estimate from the previous open area causes an error in the location estimate at the beginning of this region. Again, the standard deviation of the localization error during the second high-building region shows the instability caused by the multipath effect. The Kalman Filter finally brings the localization error back to almost the same accuracy as at the beginning of the first open-area region. However, it takes too long to minimize the error in the last open area: the vehicle has travelled almost 1.3 km before the multipath effect is eliminated.

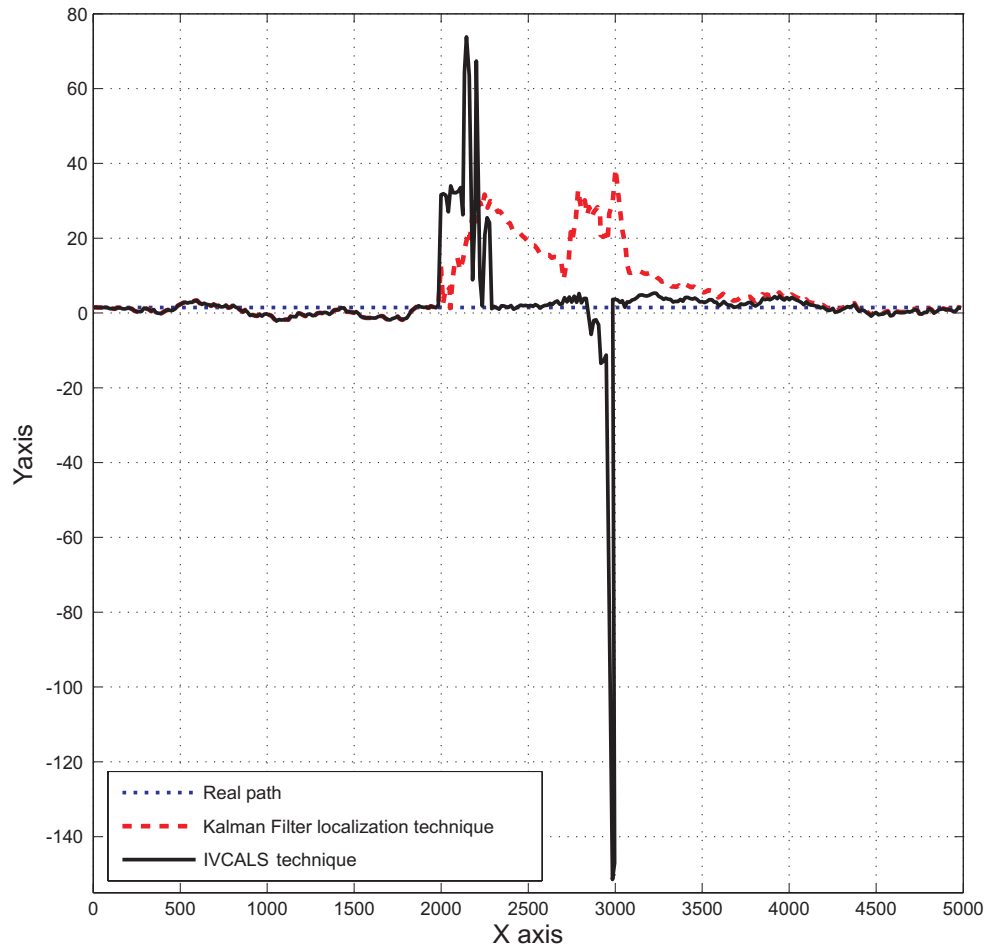


Figure 4.6: Location estimate for one vehicle in the VANET scenario; localization is implemented using the IVCALS technique. The dashed line shows the Kalman Filter technique for localization, and the solid line shows the location estimate of the IVCALS technique.

In the second experiment, the IVCALS technique, which is depicted in Figure 3.3, is used to localize vehicles in the same scenario as that shown in Figure 4.4. As mentioned in Chapter 3, this technique uses an artificial neural network to detect the multipath effect in the Kalman Filter estimate and, accordingly, performs the algorithm to improve the location estimate (Section 3.3.3). As a result, during the first open-area region, the location estimates are the same as those for the same period in the first experiment. However, in the first high-building region the difference between the location estimates of the two experiments is clear. In Figure 4.6, the dashed and dotted lines represent the Kalman Filter estimates and the real path, respectively; the solid line represents the location estimates of the IVCALS technique. Although there is no obvious improvement in the location estimates during the first high-building region, a great improvement happens in the location estimates for the following open-area region. In the second high-building region, the performance is good except for the two seconds in which the system introduces the worst two estimates in the simulations. The reason for the unexpected low accuracy in the first and second high-building regions is discussed in the Subsection 4.3.1.

Table 4.2 shows the location estimate error statistics for the second experiment. During the open-area regions of the scenario, the IVCALS technique outperforms the Kalman-Filter-only technique. Especially immediately after any high-building

region, the location estimate error became very small. Although two poor location estimates occur in the second high-building region, the mean error is less by almost 10 meters than the one produced in the first experiment. The large standard deviation in the location estimate error in the second high-building region is caused by the two errors in the location estimate during two seconds of the 29 seconds spent in that region.

### 4.3.1 Analyzing the IVCALS Technique in the Multipath Regions

In the second experiment, the algorithm for improving the location estimate introduced unexpected errors in its location estimate. The output of the algorithm is based on the optimization problem 3.13 that minimizes the error in localizing a

Table 4.2: Error statistics for the localization using IVCALS technique.

| Environment      | Distance (m) | Mean Error (m) | SD of the Error (m) |
|------------------|--------------|----------------|---------------------|
| Open area 1      | 2000         | 2.33           | 1.35                |
| High buildings 1 | 300          | 30.49          | 19.82               |
| Open area 2      | 400          | 0.86           | 0.41                |
| High buildings 2 | 400          | 14.11          | 38.63               |
| Open area 3      | 1900         | 1.75           | 0.87                |

target vehicle using other vehicles as reference points since their location estimates are more accurate than the target vehicle's. The ideal case, in which the error in the location estimate of the reference point is equal to zero, produces only one global minimum for the optimization problem.

Figure 4.7 illustrates the ideal case if the surface of the objective function of the optimization problem were to be drawn in a 3-D diagram. Figure 4.8 shows a contour depiction of the values of the objective function using different possible values for the solution of the optimization problem, which is the location of the target point. From a geometric point of view, the solution of such an optimization problem is the intersection point of three circles. These circles signify the distances between the target vehicle and the reference points: the circles are centred at the locations of the reference points, and the radius of every circle is equal to the distance between the target vehicle and the centre of that circle, as shown in Figure 4.9. Obviously, as depicted in Figure 4.8, there is only one global minimum for the optimization problem, which is the actual location of the target vehicle.

However, it is hard to find the ideal case in an experiment or even in the real world because every vehicle has an error in its location estimate. Such localization errors result in two, three, or more local minima in the optimization problem, which

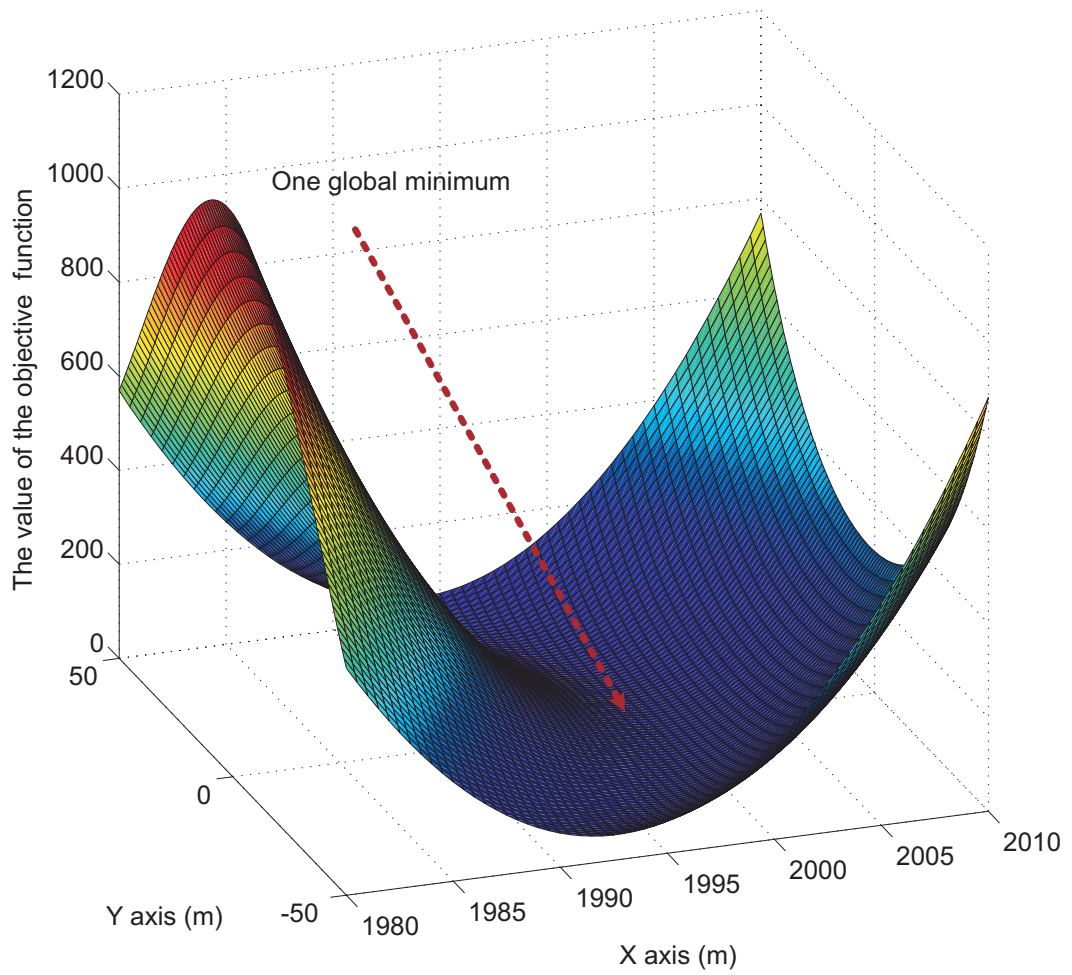


Figure 4.7: 3D representation of the optimization function in the ideal case.



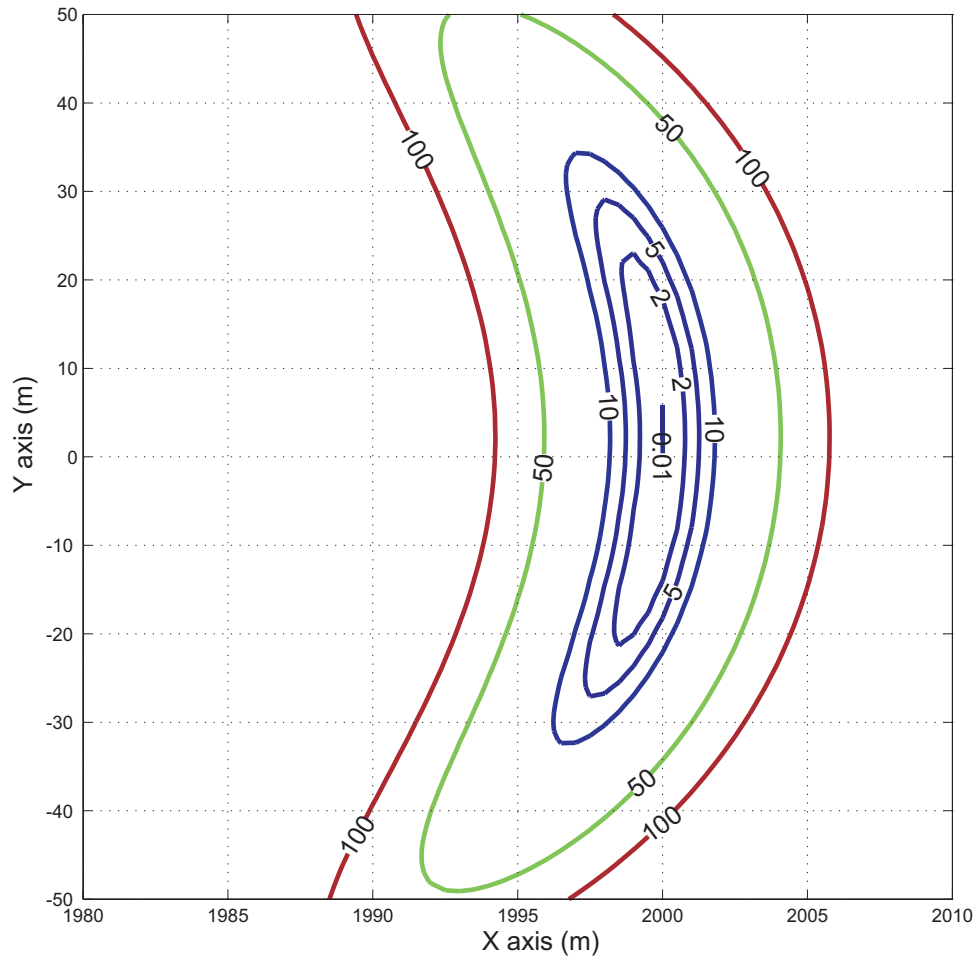


Figure 4.8: Contour representation of the optimization problem in the ideal case.

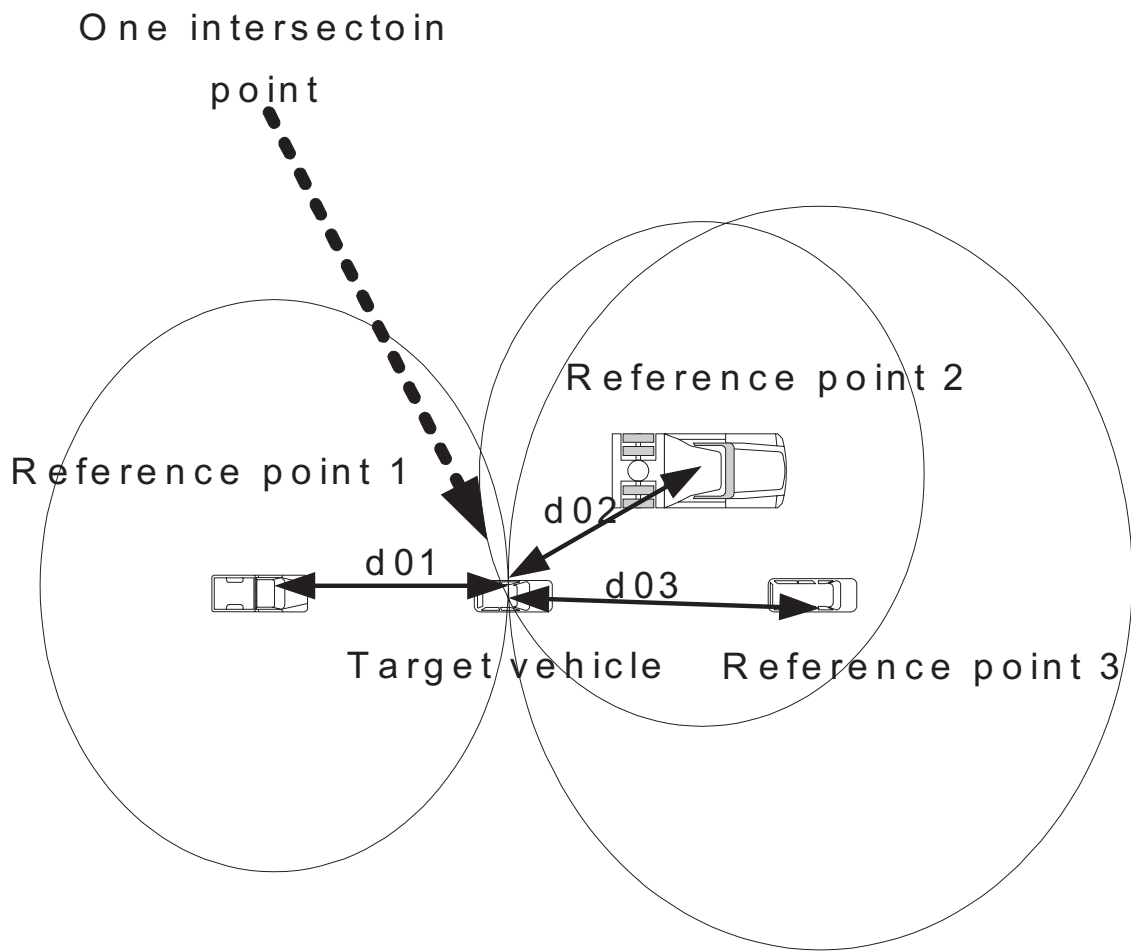


Figure 4.9: Example of the solution for the optimization problem in the ideal case.

are significant distances from the actual location of the target vehicle.

For example, Figure 4.10 shows a target vehicle trying to improve its location estimate by communicating with three other vehicles which are more accurate than the target vehicle itself, in order to make them its reference points. These reference vehicles have a degree of error in their location estimate that causes the solution of the optimization problem to fall a significant distance from the actual location of the target vehicle. Figures 4.11 and 4.12 show the two solutions for the optimization problem of this example. Often, if such an optimization problem has more than one solution, the actual location of the target vehicle is midway between these solutions [30], as depicted in Figure 4.10. Thus, if these local minima can be found, their centroid will be close to the actual location of the target vehicle.

### **4.3.2 The Adaptive IVCALS Technique**

The Nelder Mead method of solving an optimization problem is efficient because it needs neither a gradient nor Hessian computations. Thus, it is applied to the optimization problem more than once using different initial solutions. This method allows more minima to be found if there are any. As can be seen in Figure 4.10, the centroid of these minima is the location closest to the actual location of the target vehicle.

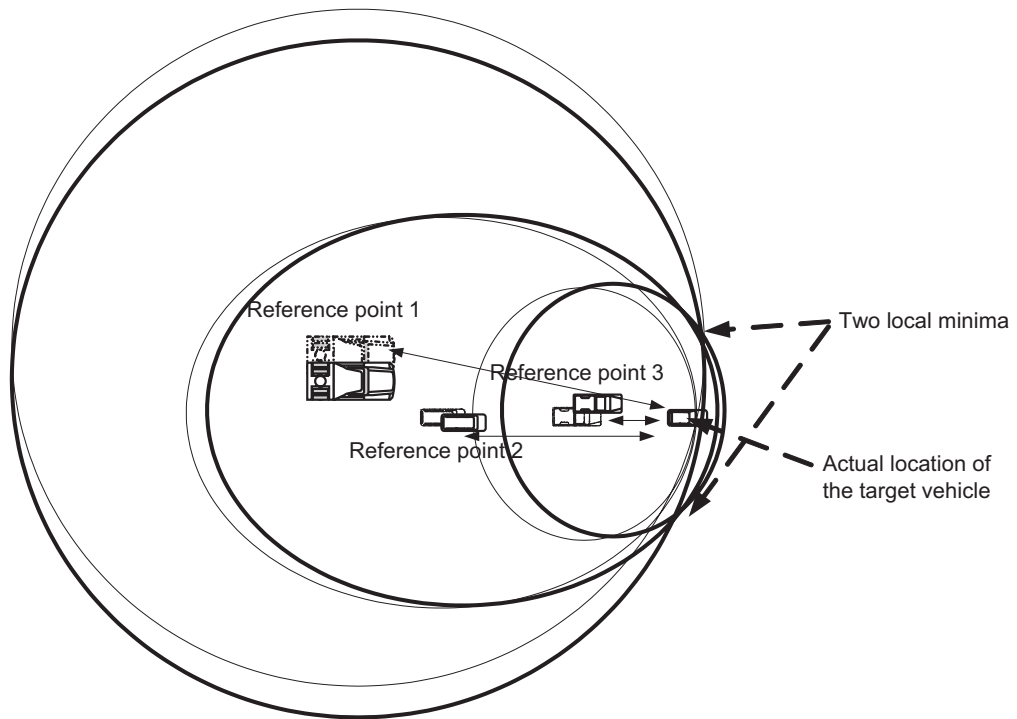


Figure 4.10: The small errors in the location estimates of the reference points create more than one solution for the optimization problem around the actual location of the target vehicle.

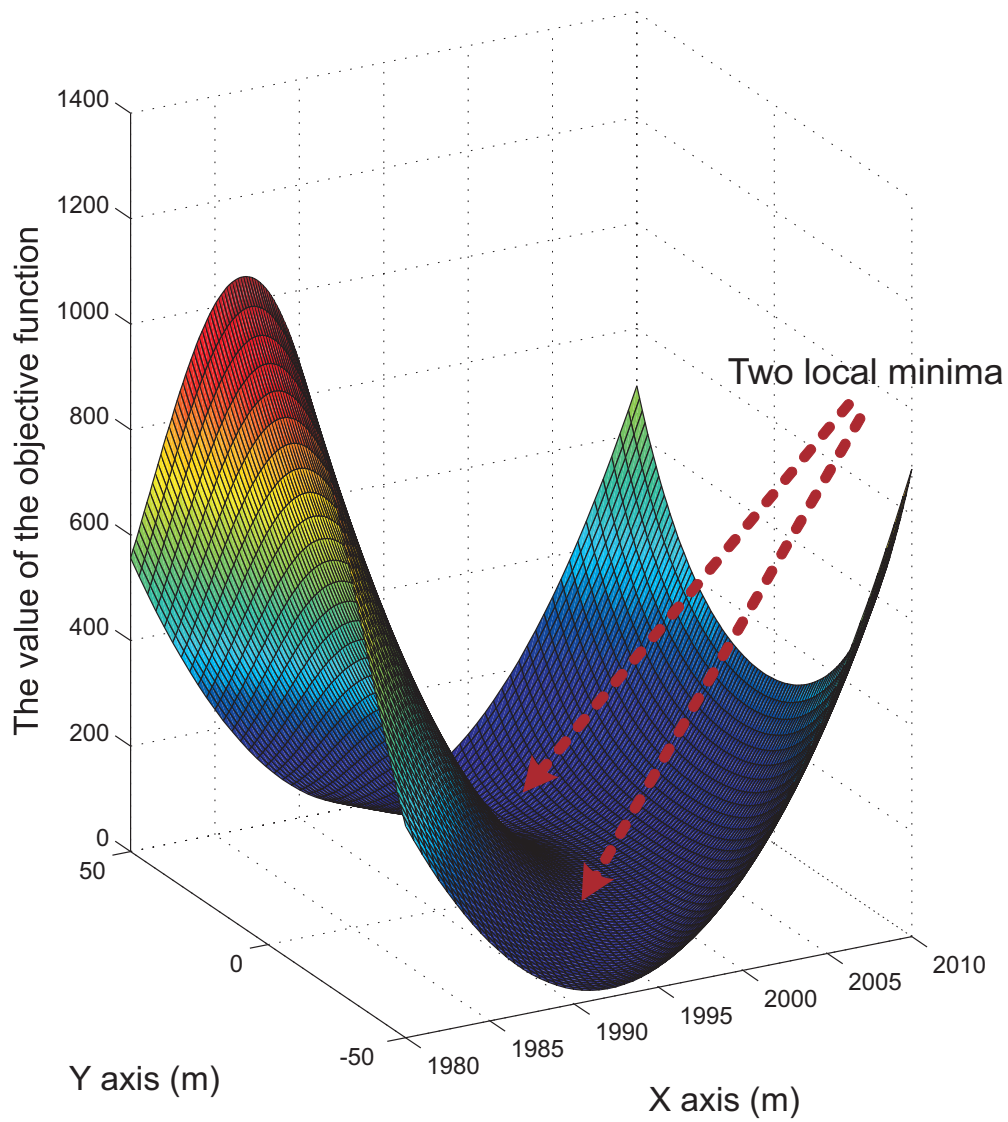


Figure 4.11: 3D representation of the optimization Problem in the real case.

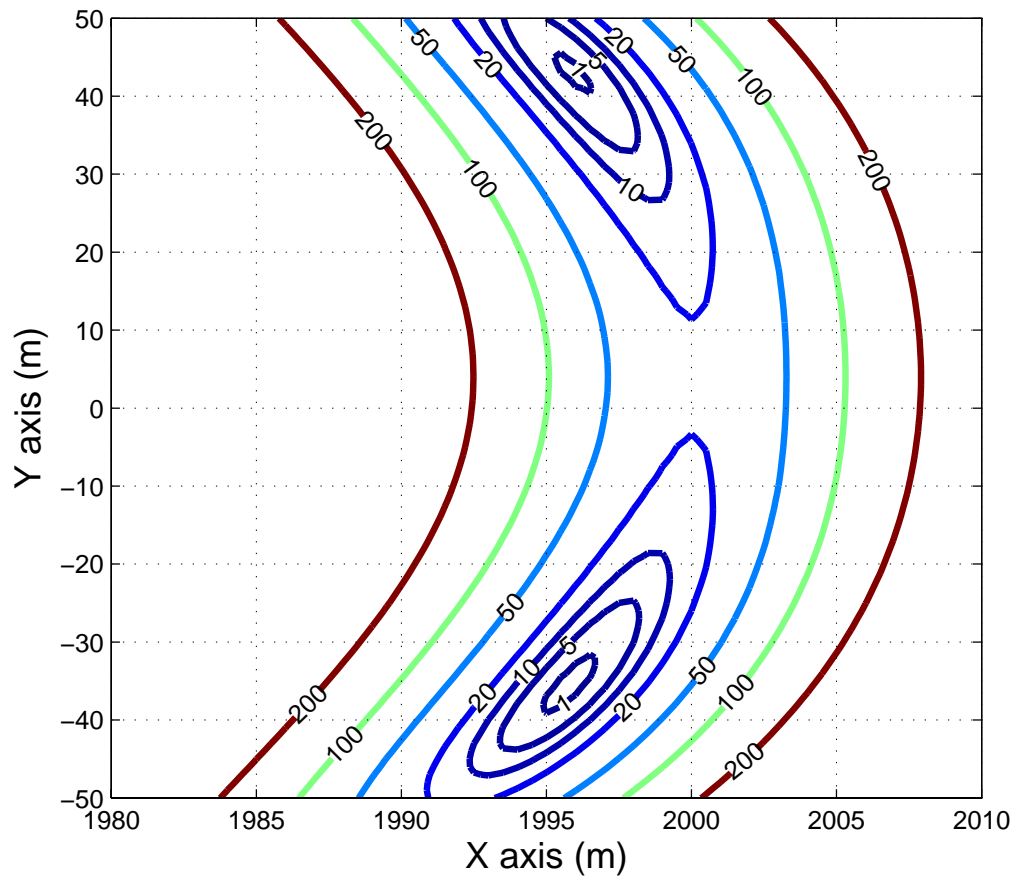


Figure 4.12: Two local minima as a solution for the optimization problem in the real case.

However, the initial solutions can not be randomly selected from the solution space because this method may lead to the same minimum point of the optimization problem. In addition, it can be seen in Figure 4.6 that the output of the Kalman Filter is always closer to the right location than the spikes that have been caused by the local minima. Thus, the area around that output is explored in order to find more local minima. This method can be implemented through the division of the space around the Kalman Filter's output into four parts and the selection of an initial solution from each part. In this way, the first initial solution for the optimization problem is the output of the Kalman Filter. The output of the Kalman Filter is then used as a reflection point in order to find new other initial solutions. If all the initial solutions lead to the same minimum point, then there is only one global minimum solution, which is close to the actual location of the target vehicle. Otherwise, the result will be a number of local minima around the actual location of the target vehicle, which can then be found by computing the centroid of these minima.

Figure 4.13 shows how the adaptive IVCALS technique behaves when it is searching for the local minima for the previous example shown in Figure 4.12. The first initial solution  $(\tilde{X})$  is the output of the Kalman Filter in which the optimization technique finds the local minimum at the top of the figure  $(\hat{X}_1)$ . The second ini-

tial solution  $(\tilde{X}_2)$  leads the optimization technique to the previous local minimum  $(\hat{X}_1)$ . However, the third and fourth initial solutions  $(\tilde{X}_3, \tilde{X}_4)$  lead the optimization technique to the local minimum at the bottom of the figure  $(\hat{X}_2)$ .

The following equation depicts how the initial solutions can be determined using the first local minimum  $\hat{X}_1$  and the output of the Kalman Filter  $\tilde{X}$ :

$$\tilde{X}_{i+1} = \tilde{X} + \mathbf{J}(i) (\hat{X}_1 - \tilde{X})$$

where

$i = 1, 2, 3$

$\tilde{X}_i$  are the initial solutions

$\mathbf{J}(i)$  is an  $i \times 90^\circ$  rotation matrix

The last step is the determination of the location estimate by the computation of the centroid of the local minima.

## 4.4 The Results of the Adaptive IVCALS Technique

The third experiment follows the same scenario as the previous experiments, with the added feature of the adaptive IVCALS technique being implemented in every vehicle in VANET. Figure 4.14 shows the location estimate of the same vehicle that was used in Figure 4.6. In Figure 4.14, the adaptive IVCALS technique is



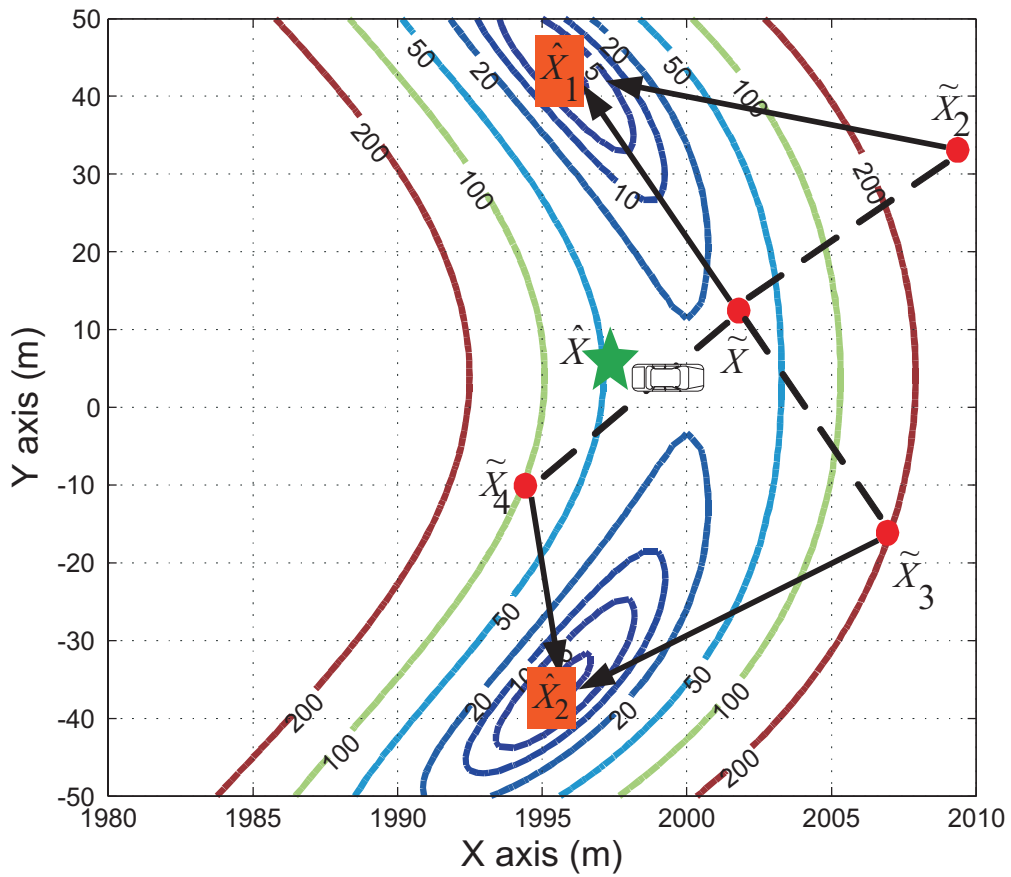
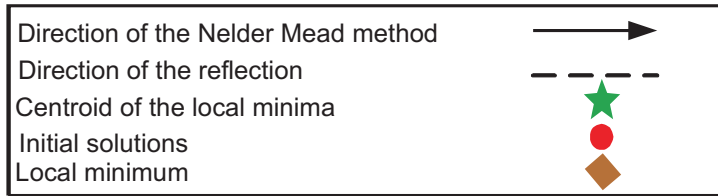


Figure 4.13: The adaptive IVCALS technique searches for the local minima and computes the centroid point.

marked by a solid line, the IVCALS technique is marked by a dash-and-dot line, the Kalman Filter technique is marked by a dashed line, and the real path is marked by a dotted line. It can be seen in the Figure that the adaptive IVCALS technique outperforms both the Kalman filter and the IVCALS techniques. Table 4.3 shows the statistics for the localization errors using the adaptive IVCALS technique.

#### 4.4.1 Comparison of the Techniques and Experiments

Figures 4.15 and 4.16 show a comparison of the three techniques. In Figure 4.15, the vertical axis represents the standard deviation of the localization error and the horizontal axis represents from left to right the regions that the vehicle traverses over the 5 km. The performance of the techniques are similar in the first open-area region. With the IVCALS technique, the standard deviation becomes high in the high-building regions; however, the mean error of the localization improves

Table 4.3: statistics for the localization using the adaptive IVCALS technique.

| Environment      | Distance (m) | Mean Error (m) | SD of the Error (m) |
|------------------|--------------|----------------|---------------------|
| Open area 1      | 2000         | 2.33           | 1.35                |
| High buildings 1 | 300          | 6.55           | 6.31                |
| Open area 2      | 400          | 0.88           | 0.41                |
| High buildings 2 | 400          | 7.22           | 6.60                |
| Open area 3      | 1900         | 2.39           | 1.52                |

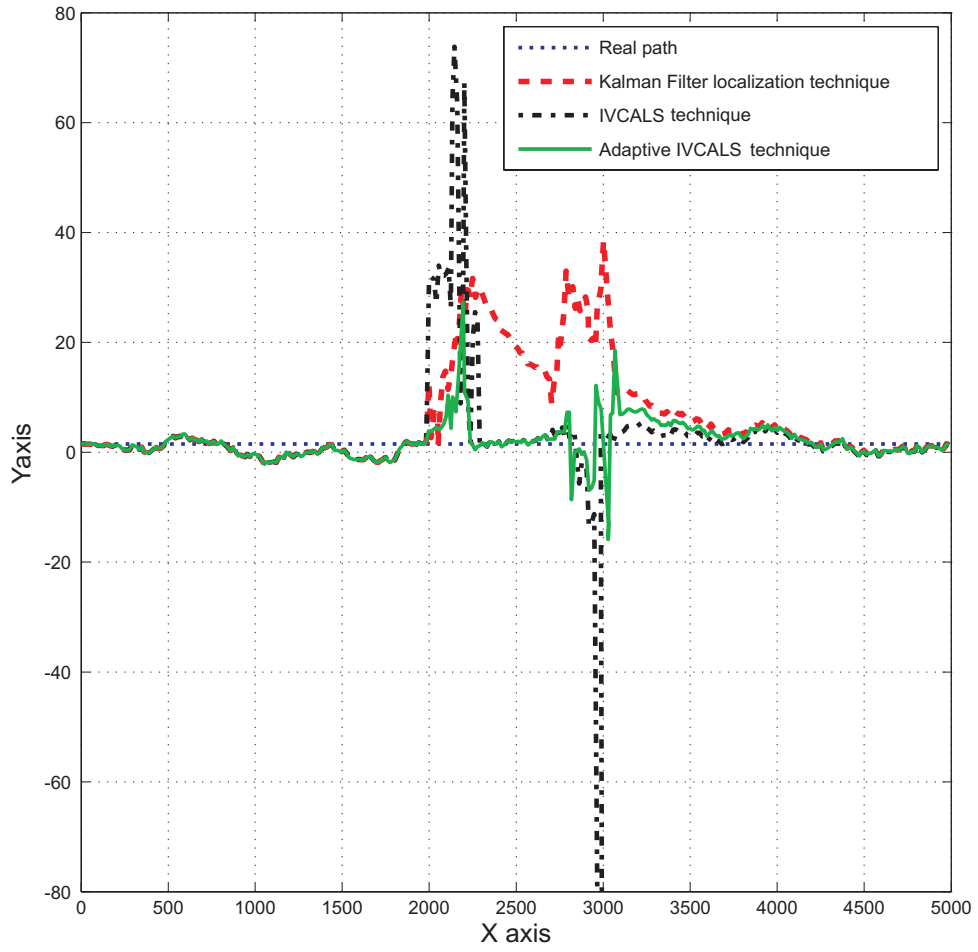


Figure 4.14: Location estimate for one vehicle in the VANET scenario; the localization is implemented using the adaptive IVCALS technique.

in the second high-building region, as shown in Figure 4.16. The increase in the standard deviation is caused by the spikes shown in Figure 4.6, which are reduced with the adaptive IVCALS technique. In the second open-area region, both the IVCALS and the adaptive IVCALS techniques perform much better than the Kalman Filter technique. Generally, the adaptive IVCALS technique performs better than the Kalman Filter technique and is more stable than the IVCALS technique since its standard deviation is relatively small during both the open-area regions and the high-building regions.

Figure 4.17 shows a comparison between the IVCALS technique and the adaptive IVCALS technique. The comparison is based on the percentage of the time the new techniques outperform the Kalman Filter technique during the simulation period. The horizontal axis represents ranges of percentages of 10% each, from 0% to 100%. The vertical axis represents the number of vehicles that have performances within each specific 10% range. For example, during 20% to 30% of the simulation time seven vehicles perform better when they use the IVCALS technique than when they use the Kalman Filter technique. On the other hand, during 20% to 30% of the simulation time three vehicles perform better when they use the adaptive IVCALS technique than when they use the Kalman Filter technique. It can be seen in Figure 4.17 that when the adaptive IVCALS technique is used the number of

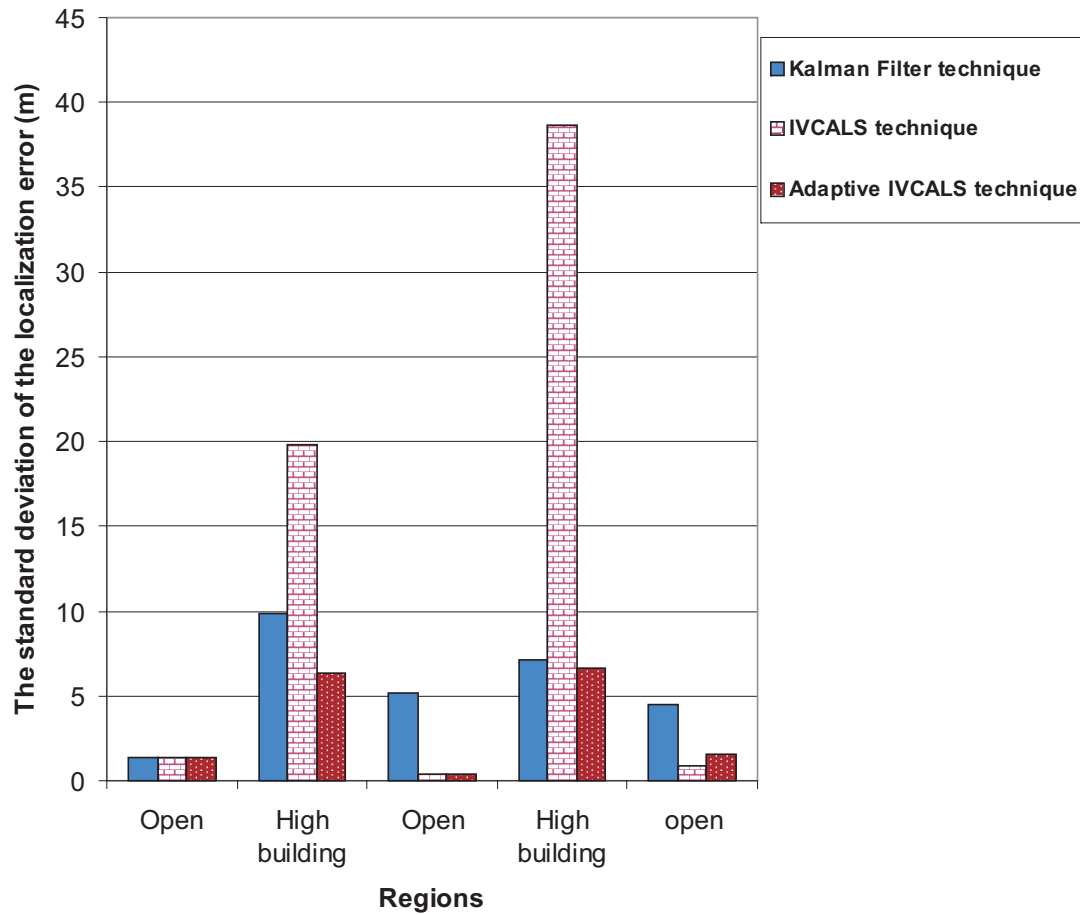


Figure 4.15: Comparison of the three techniques: the standard deviation of the localization error for the three techniques is shown relative to the environments the vehicles pass through from left to right.

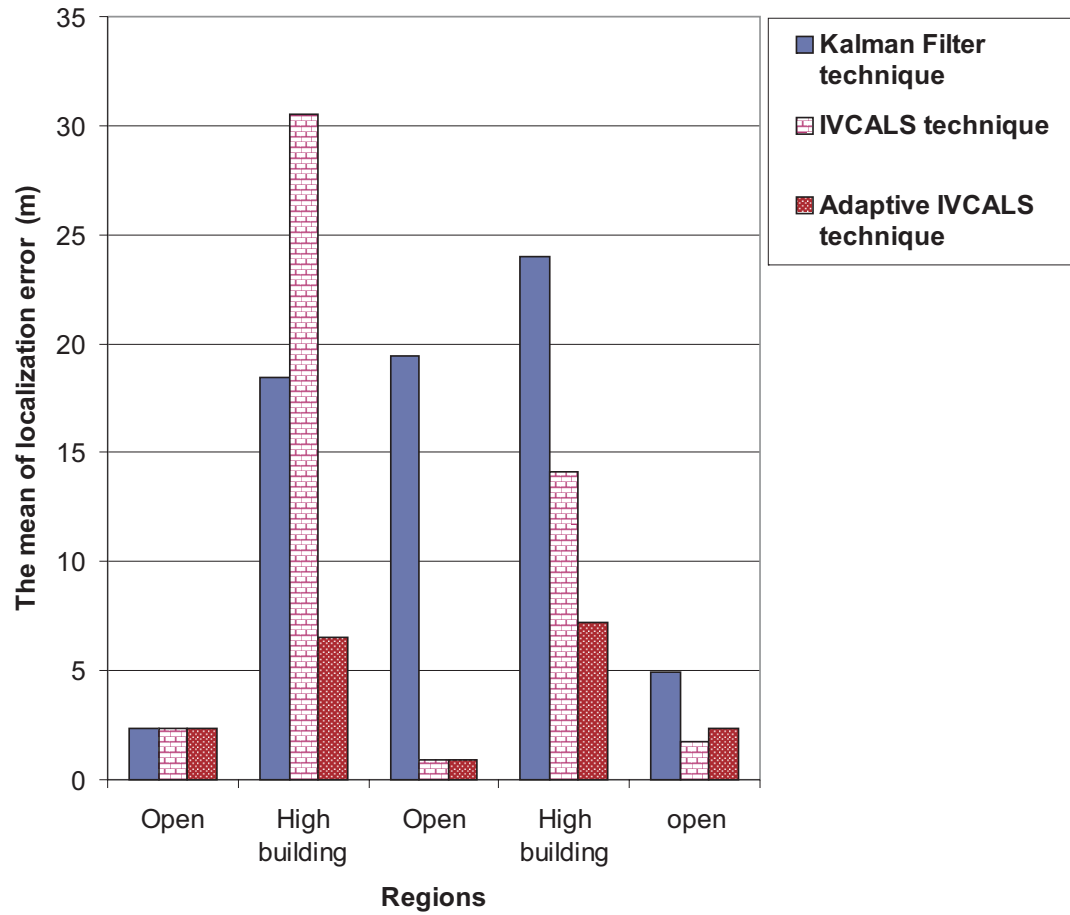


Figure 4.16: Comparison of the three techniques: the mean localization for the three techniques versus the environments vehicles pass through error of the localization error for the three techniques versus the environments pass through from left to right.

vehicles which improve their performance between 90% and 100% of the simulation time is increased dramatically from three to 14. During 40% to 50% of the simulation time, 23 vehicles, the most in any percentage range, perform better when they use the IVCALS technique than when they use the Kalman Filter technique. Using the IVCALS technique, most of the vehicles perform better than when they use the Kalman Filter technique. In addition, both new techniques outperform the Kalman Filter during all the percentage ranges beyond 20% of the simulation time.

However, if the new techniques outperform the Kalman Filter during just 20% of the simulation time, that performance measure does not reflect how much the new techniques increase the error over the Kalman Filter error in the remaining 80% of the time. For this reason, the summation of the errors during the experiment is calculated for each technique on every vehicle. Then the summation of the errors is averaged among vehicles in the same percentage range of the simulation time. The ratio between the summation of the Kalman Filter's errors and the summation of the new techniques' errors is the other performance measure. Figure 4.18 depicts the two measures superimposed on one another.

In Figure 4.18, the worst case using the adaptive IVCALS technique is obtained when the technique outperforms the Kalman Filter during 20% to 30% of the sim-

ulation time. However, for the 20%-30% range the ratio between the total location estimate errors using the Kalman Filter technique and the one using the adaptive IVCALS technique is 1.07, which means that the total estimation error is almost the same for the two techniques. In other words, the adaptive IVCALS technique improves the location estimate in 20%-30% of the simulation time, which compensates for the errors in the location estimate during the remaining 70-80% of the simulation time. Moreover, the ratio increases as the time increases: when vehicles use the adaptive IVCALS technique, the ratio is more than 2 for the 90%-100% range.



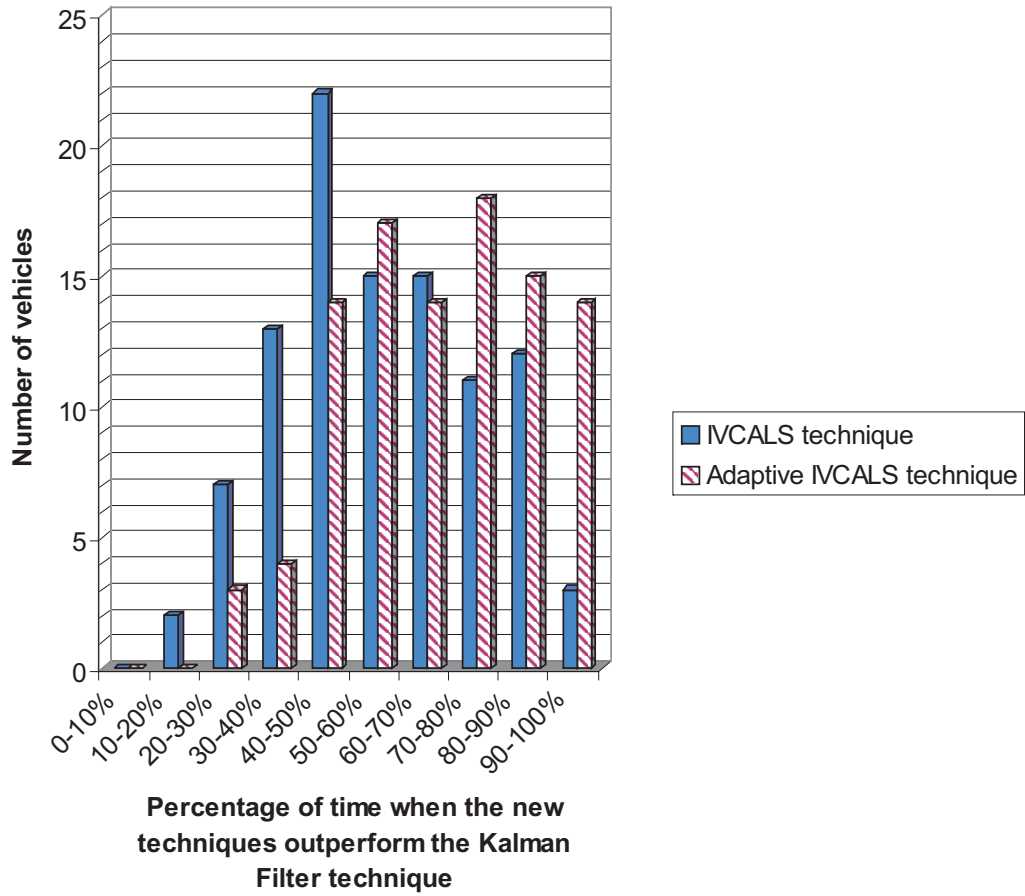


Figure 4.17: Comparison between the IVCALS and the adaptive IVCALS techniques and how they improve the location estimate relative to the Kalman Filter technique.

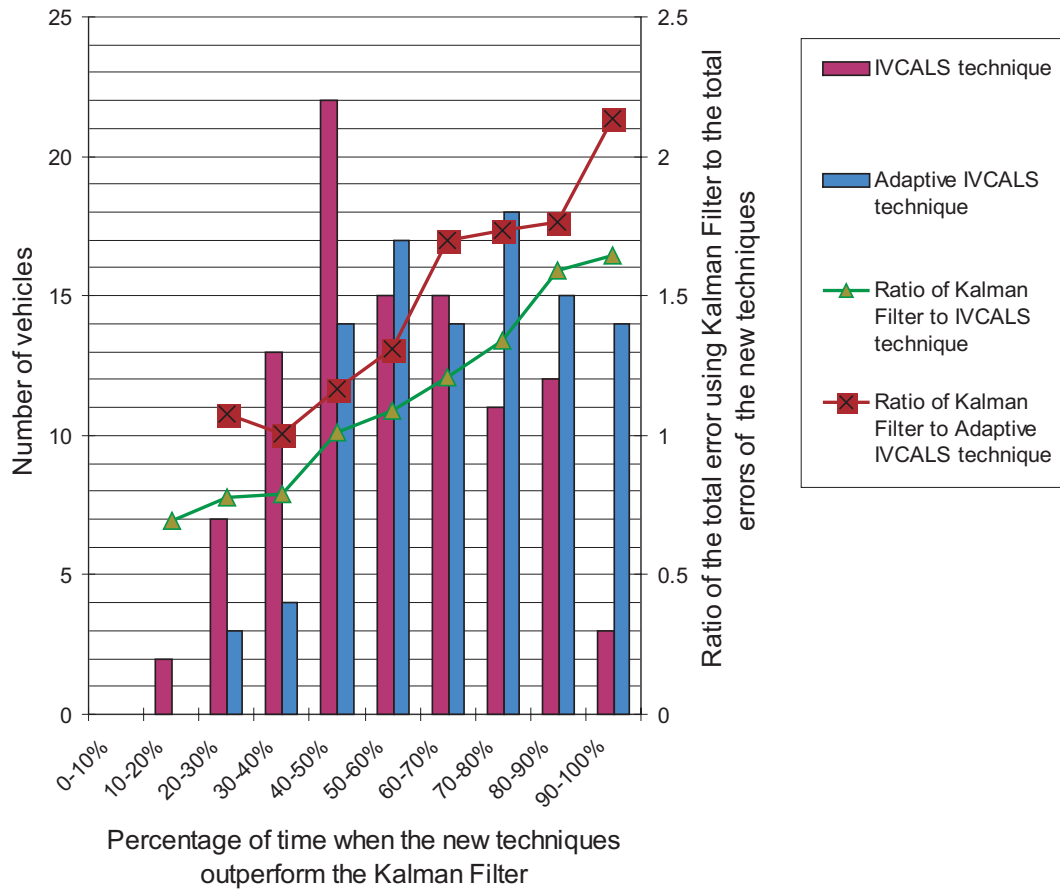


Figure 4.18: Performance measures. The ratios of total error in the location estimate using the Kalman Filter technique to those using the new techniques are superimposed on the time performance measure.

# Chapter 5

## Conclusions and Future Work

In this thesis, new techniques have been proposed for improving the accuracy of the location estimate in VANET. This chapter summarizes these techniques and suggests the future work.

### 5.1 Conclusions

The techniques and algorithms in this thesis have been developed to be used in VANET for localization. Vehicles in VANET often use GPS receivers to localize themselves; however, the accuracy of the GPS receiver's location estimate is not reliable when the satellite signal is completely lost or distorted by trees, high buildings, or tunnels. The absence of satellite signals has been studied in much of the research and a Kalman Filter has been employed in order to integrate the GPS measurements with other measurements, such as the INS measurements, and to

overcome the outage of the satellite signals. however, the distortion of the satellite signal still causes misleading information for the localization systems in the vehicles.

In the new techniques, the GPS receiver measurements are integrated with the INS measurements using a Kalman Filter because it has been proven that the Kalman Filter can fuse sensed data and obtain a minimum mean square error. To avoid the distortion of the satellite signal caused by the multipath effect, a classifier has been added in order to detect whether the satellite signal is affected by the multipath signals that the system is receiving. This classifier was designed using an Artificial Neural Network, which has been trained using samples of the satellite signals. once the classifier produces a result, the new techniques decide whether to take the output of the Kalman Filter as the final output or to optimize the Kalman Filter's output using the proposed algorithms.

When the output from the Kalman Filter is distorted in a target vehicle, the first step is to use the facility of the communication among the vehicles in VANET to determine the distance between the target vehicle and all of its neighbours. From the information received, the target vehicle obtains the locations of its neighbours, according to their estimates, and to their uncertainty measure, which has been built up chronologically. Next, based on the uncertainty measure, the target ve-

hicle chooses the neighbours with the best location estimates and uses them as reference points. Then, all the pieces of information obtained are formulated into a least squares optimization problem in order to improve the location estimate of the target vehicle.

Although the above algorithm outperformed the Kalman Filter method of vehicle localization, some poor location estimates showed up in the simulation for just a few seconds. This problem has been analyzed and modifications to the proposed technique have been developed so that an accurate location can be estimated through the finding of more than one local minimum if there are any. The target vehicle estimate is found from the computation of the centroid of the local minima. The simulations showed great improvement in the estimate of the location after the modification had been implemented.

The VANET simulation was comprised of 100 vehicles travelling on a 5 km stretch of road in urban area, in which they pass through different environments, such as open areas and high-building areas, for different distances. The simulation results, when vehicles were using the Adaptive IVCALS technique, are concluded as follows:

- The Adaptive IVCALS technique outperformed the Kalman Filter for 14 vehi-

cles during more than 90% of the simulation time and minimized the location estimate error by 53% on average.

- In 64 vehicles, the Adaptive IVCALS technique outperformed the Kalman Filter in durations of 50% to 90% of the simulation time, and it minimized the location estimate error by 37.5% on average.
- In 14 vehicles, the Adaptive IVCALS technique outperformed the Kalman Filter in durations of 40% to 50% of the simulation time, and it minimized the location estimate error by 13.8% on average.
- In just 9 vehicles, the Adaptive IVCALS technique outperformed the Kalman Filter in durations of 20% to 40% of the simulation time, and it produced almost the same amount of location estimate error on average.

In other words, vehicles in VANET have a high probability of greatly improving their location estimates in urban areas using the Adaptive IVCALS technique. In the worst case, just a few vehicles will have the same error as that caused by the ordinary techniques such as the Kalman Filter.

## **5.2 Future Work**

Implementing the new techniques in the real world seems to be a promising possibility. However, a number of issues need to be addressed.

### **5.2.1 3D Coordinates**

The work in this thesis tackled the localization problem based on an assumption that vehicles are moving on a plan topography, represented by two coordinates. To be implemented in the real world, the new techniques need to be adapted so that they can represent locations in three dimensions.

### **5.2.2 MAC and Network Layers**

Although the new techniques do not require a great deal of data exchange among nodes in VANET nor do they require communication that needs more than one hop, a study needs to determine the best communication protocols in the physical, MAC , and Network layers that are suitable for VANET.

### **5.2.3 Embedded systems' design**

The new localization algorithms are currently implemented in MATLAB. The next step is to convert the MATLAB codes to C in order to facilitate the use of these

techniques in embedded systems or real VANET implementations.



# Bibliography

- [1] FCC. Enhanced wireless 911 services.  
[http://www.fcc.gov/Bureaus/Wireless/News\\_Releases/1999/nrwl9040.txt](http://www.fcc.gov/Bureaus/Wireless/News_Releases/1999/nrwl9040.txt).
- [2] [www.car-accidents.com](http://www.car-accidents.com).  
<http://www.car-accidents.com/pages/stats.html>.
- [3] T. He, J. A. Stankovic, C. Lu, and T. Abdelzaher. Speed: A stateless protocol for real-time communication in sensor networks. In Proceedings of the 23rd International Conference on Distributed Computing Systems, pages 46–55, Washington, DC, USA, 2003. IEEE Computer Society.
- [4] A. Capone, I. Filippini, L. Fratta, and L. Pizziniaco. *Receiver Oriented Trajectory Based Forwarding*. Springer-Verlag Berlin Heidelberg 2006, lecture notes in computer science, lncs 3883 edition, 2006.
- [5] Swades De, Antonio Caruso, Tamalika Chaira, and Stefano Chessa. Bounds on hop distance in greedy routing approach in wireless ad hoc networks.
- [6] Jeffrey Hightower and Gaetano Borriello. Location systems for ubiquitous computing. *IEEE Computer*, 34(8):57–66, August 2001.
- [7] W. W. Kao. Integration of gps and dead-reckoning navigation systems. In *Proc. Vehicle Navigation and Information Systems Conference*, pages 635 – 643, 1991.

- [8] D. Bouvet and G. Garcia. Improving the accuracy of dynamic localization systems using rtk gps by identifying the gps latency. In *Proceedings of the 2000 IEEE, International Conference on Robotics & Automation*, San Francisco, CA April 2000, 2000.
- [9] Qi. Honghui and J. B. Moore. Direct kalman filtering approach for gps/ins integration. *IEEE Transactions on Aerospace and Electronic Systems*, 38(2):687 – 693, 2002.
- [10] Rashad Sharaf, Aboelmagd Noureldin, Ahmed Osman, and Naser El-Sheimy. Online ins/gps integration with a radial basis function neural network. *IEEE A&E SYSTEMS MAGAZINE*, MARCH 2005.
- [11] Shahram Rezaei and Raja Sengupta. Kalman filter based integration of dgps and vehicle sensors for localization. In *Proceedings of the IEEE, International Conference on Mechatronics & Automation*, Niagara Falls, Canada, July 2005.
- [12] www.trimble.com. <http://www.trimble.com/gps/whygps.shtml>.
- [13] J. L. Leva. An alternative closed-form solution to the gps pseudo-range equations. *Aerospace and Electronic Systems, IEEE Transactions*, 32(4):1430 – 1439, 1996.
- [14] J. Hoshen. The gps equations and the problem of apollonius. *Aerospace and Electronic Systems, IEEE Transactions*, 32(3):1116 – 1124, 1996.
- [15] Geocommunity website - spacialnews.  
<http://spatialnews.geocomm.com/features/sa/gps.html>.
- [16] Javad navigation systems inc.  
<http://www.javad.com/index.html?/jns/gpstutorial/Chapter3.html>.

- [17] S. Capkun, M. Capkun, M. Hamdi, and J-P Hubaux. Gps-free positioning in mobile ad hoc network. Hawaii International Conference on System Sciences, 2001.
- [18] S. Venkatraman, Jr. J. Caffery, and H. R. You. Location using los range estimation in nlos environments. In *Vehicular Technology Conference, 2002. VTC Spring 2002. IEEE 55th*, volume 2, pages 856 – 860, May 2002.
- [19] Bao Long Le, Kazi Ahmed, and Hiroyuki Tsuji. Mobile location estimator with nlos mitigation using kalman filtering. In *Wireless Communications and Networking, 2003. WCNC 2003. 2003 IEEE*, volume 3, pages 1969 – 1973. Asian Inst. of Technol., Thailand, March 2003.
- [20] M.P. Wylie and J. Holtzman. The non-line of sight problem in mobile location estimation. In *Universal Personal Communications, 1996. Record., 1996 5th IEEE International Conference on*, volume 2, pages 827 – 831, Cambridge, MA, September 1996.
- [21] Jr. James J. Caffery and Gordon L. Stber. Overview of radiolocation in cdma cellular systems. *IEEE Communications Magazine*, 36(4):38 – 45, April 1998.
- [22] Abderrahim Benslimane. Localization in vehicular ad-hoc networks. In *Proceedings of the 2005 Systems Communications (ICW'05)*, 2005.
- [23] Eun-Hwan Shin. Accuracy improvement of low cost ins/gps for land applications. Master's thesis, THE UNIVERSITY OF CALGARY, 2001.
- [24] J. Rankin. An error model for sensor simulation gps and differential gps. *Position Location and Navigation Symposium*, 11(15):260–266, April 1994.

- [25] M.E. Cannon and G. LaChapelle. Analysis of a high-performance c/a-code gps receiver in kinematic mode. *Navigatin: Journal of the Institute of Navigation*, 39(3):285–300, Fall 1992.
- [26] Liang Cheng Yuecheng Zhang. Place: Protocol for location and coordinate estimation—a wireless sensor network approach. *ELSEVIER Computer Networks*, 46:679–693, 2004.
- [27] Yinyu Ye Pratik Biswas. Semidefinite programming for ad hoc wireless sensor network localization. Berkeley, CA, April 2004.
- [28] Patrick Y. C. Hwang Robert Grover Brown. *Introduction To Random Signals and Applied Kalman Filtering*. John Wiley & Sons, thidr edition, 1997.
- [29] Jorge Nocedal and Stephan J. Wright. *Numerical Optimization*. Springer, second edition, 2000.
- [30] Koen Langendoen and Niels Reijers. Distributed localization in wireless sensor networks: a quantitative comparison. *Elsvier, Computer networks*, (43):499–518, 2003.